




An overview of electrochemical advanced oxidation processes applied for the removal of azo-dyes

Lucas Destefani Paquini^{1,2} · Lília Togneri Marconsini² · Luciene Paula Roberto Profeti² · Othon Souto Campos² · Demetrius Profeti² · Josimar Ribeiro¹ 

Received: 12 July 2022 / Revised: 28 November 2022 / Accepted: 10 January 2023 / Published online: 30 January 2023
© The Author(s) under exclusive licence to Associação Brasileira de Engenharia Química 2023

Abstract

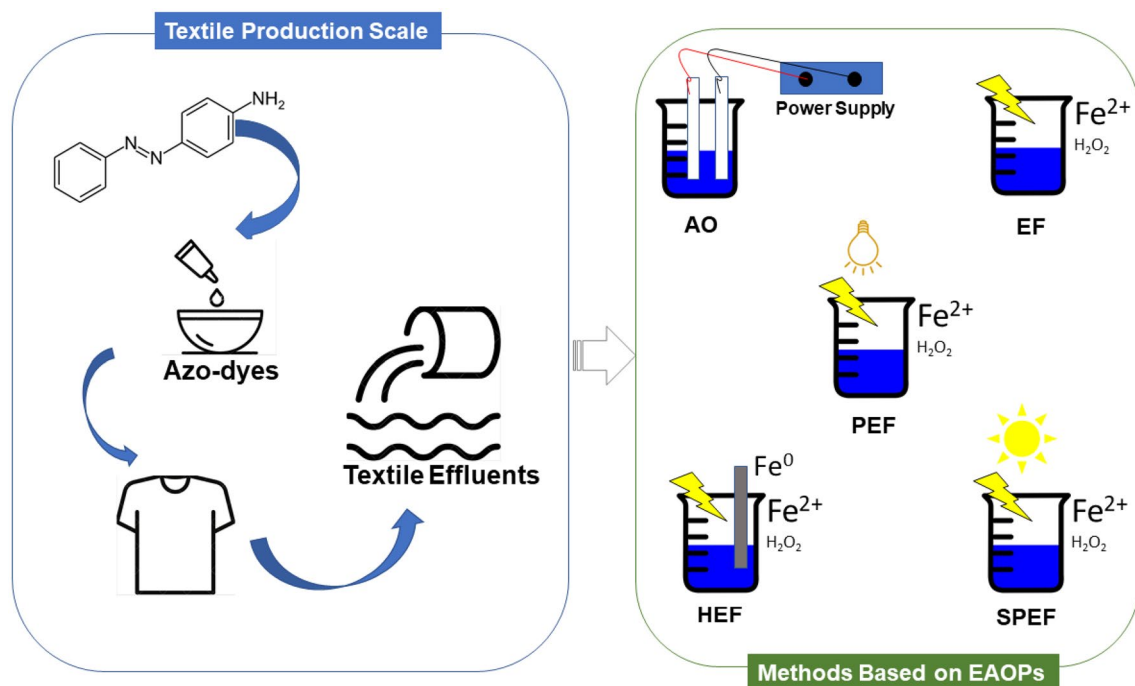
The production, commercialization and use of dyes by industries has increased significantly over the last few decades. The frequent release of liquid effluents into water bodies, which contain high loads of toxic contaminants, such as dyes and pigments, represents a substantial risk to aquatic biota, and negative influence on wildlife as a whole. Among the main dyes used in the textile industries, Azo-dyes are considered the group with the largest usability for dyeing jeans, cotton, and polyester. Considering their dangerous effect on the environment, the development of methods for the removal of these species has become forceful nowadays. The processes of oxidative degradation are considered highly efficient, especially when electrochemical advanced oxidation processes (EAOPs) are applied, such as electrochemical oxidation (EO), electro-Fenton (EF), and Heterogeneous Electro-Fenton (HEF), Photoelectro-Fenton (PEF), and Solar Photoelectro-Fenton (SPEF). Thereby, this review presents a state of the art based on these electrochemical removal technologies, taking into account their applications in some pH conditions, different types of electrodes, and different mechanisms of electro-generation of mediators when it is necessary. Furthermore, our review addresses some methods of monitoring the extent of electrochemical reactions involved in EAOPs and presents and suggests different applications in the scaling-up spectrum for pilot plant systems, discussing the issues of efficiency and feasibility for possible implementation later.

✉ Josimar Ribeiro
josimar.ribeiro@ufes.br

¹ Laboratório de Pesquisa e Desenvolvimento em Eletroquímica (LPDE), Department of Chemistry, Center of Exact Sciences, Federal University of Espírito Santo, Campus Goiabeiras, Av. Fernando Ferrari, Vitória, ES 29075-910, Brazil

² Department of Chemistry and Physics, Federal University of Espírito Santo, Alegre, ES 29500-000, Brazil

Graphical abstract



Keywords Environmental · Removal · Azo-dye · EAOPs · Scale-up

Introduction

Over the last few decades, the degradation of water resources caused by industrial activity has become a major risk factor for the environment (Guimarães et al. 2020). This problem arises from the discharge of untreated wastewater, which contains high loads of highly toxic contaminants, thus causing a great impact on the environment (Rajkumar and Kim 2006; Steter et al. 2016). In textile industries, water is used as a vehicle for chemical products in fiber processing and the removal of excess species is considered undesirable for the final product (Guaratini and Zanoni 2010). Among the chemical products used in textile production, dyes and pigments stand out, which are considered the most harmful substances present in industrial liquid effluent emissions.

According to historical estimates, purple-blue was the first synthetic dye to be used in textile production, and until the mid-1970s, around 60% of the total production of this industrial branch was of synthetic origin (Valero et al. 2014). On the market, there is a wide variety of dyes available, being produced annually around 100 to 250 tons all over the world (Adedayo et al. 2004; Waghmode et al. 2011). In the last 50 years, the production and sale of textile dyes have made a gigantic leap. Ramya et al. (2017) report that, in the year 2017, textile industries produced about US\$ 35 billion,

which is equivalent to 16% of the total production value of the European manufacturing industry (Ramya et al. 2017). In addition, among the industrial branches that most pollute the environment, the textile branch has a contribution share of around 27–30%. From an environmental point of view, the removal of color from the textile-washing bath is one of the biggest problems in the sector. It is estimated that around 15% of the world's production of dyes is lost to the environment during their synthesis, processing, or application (Kyzioł-Komosińska et al. 2018).

There is a range of dyes commonly used in industry, with azo-dyes being the class of dyes widely used in dyeing jeans, cotton, and polyester. According to Vasconcelos et al. (2016) due to their complex chemical structure, these types of dyes are resistant to disaggregation/degradation by chemical, physical or biological treatments (Vasconcelos et al. 2016; Tomaz et al. 2022). Due to their high solubility in water, azo-dyes manage to change their color and turbidity, even at low concentrations, promoting eutrophication processes in aquatic bodies (Coura et al. 2020). As long-term exposure to these contaminants promotes mutagenic and carcinogenic effects on human beings, their removal from industrial effluents has become a matter of great urgency, given their harmful effects on life (Eren and Acar 2007; Tunç et al. 2009).

In order to minimize the impacts caused by the presence of azo-dyes in tailing, some effluent treatment methods such as precipitation, followed by coagulation, membrane filtration, oxidative processes, and adsorption have been developed (Eren and Acar 2007; Pham et al. 2021). Advanced oxidative processes (AOPs) are considered green methodologies applied to the degradation of organic matter, aiming at it reaching a mineralization stage. In this process, hydroxyl radicals ($HO\cdot$) are used as active reagents, which are generated in situ during the procedure (Titchou et al. 2021a). Electrochemical Advanced Oxidation Processes (EAOPs) have been widely used in the field of wastewater treatment, showing high efficiency in removing persistent contaminants, such as azo-dyes (Oller et al. 2011; Brillas 2020). In this method, hydroxyl radicals are generated in an electrolytic system from the addition of external catalysts, as occurs in purification processes by Electro-Fenton (EF) or by Electrochemical Oxidation (EO).

In general, the amount of catalysts used in EAOPs is smaller compared to AOPs. In specific cases, such as EF, reagents are generated in situ during the phenomenon of electrolysis, with the formation of hydrogen peroxide from the cathodic reduction of dissolved oxygen (Titchou et al. 2021a). These oxidative processes are adopted for cases where the contaminants present in effluents have a chemical oxygen demand (COD) in the order of $0.1\text{--}5.0\text{ g L}^{-1}$. One of the main points of interest in the use of these oxidative techniques is the biodegradability of contaminants and the purification of aqueous bodies containing dyes and heavy metals (Nidheesh et al. 2020). Furthermore, these techniques have the differential of operating under ambient temperature and pressure conditions, without the need to add auxiliary reagents. As they are modular techniques, AOPs and EAOPs allow the combination of several other techniques to the oxidative process, such as for example, coagulation or adsorption, to complete treatments and increase the purity index of the aqueous body. Although very efficient, the EAOPs presents as the main problem the application and/or cycle limits, in addition to the work electrodes suffering from adsorption processes of a chemical and irreversible nature when it operates in reduction reactions, making it unfeasible and/or reducing its useful life due to the blocking of the electrode surface of the electrodes (Oller et al. 2011; Sirés et al. 2014; Roshini et al. 2017).

EAOPs can be divided into different techniques, the most common are direct and indirect Electrochemical Oxidation (EO), Electro-Fenton (EF), Heterogeneous Electro-Fenton (HEF), Photoelectro-Fenton (PEF), Solar Photoelectro-Fenton (SPEF), and Electro-Coagulation (EC). Generally, the efficiency of EAOPs depends on some parameters, such as the type of electrode, the nature of the support, the type of coating, and the preparation method (Comninellis and Vercesi 1991). Furthermore, an EAOPs also depends on the

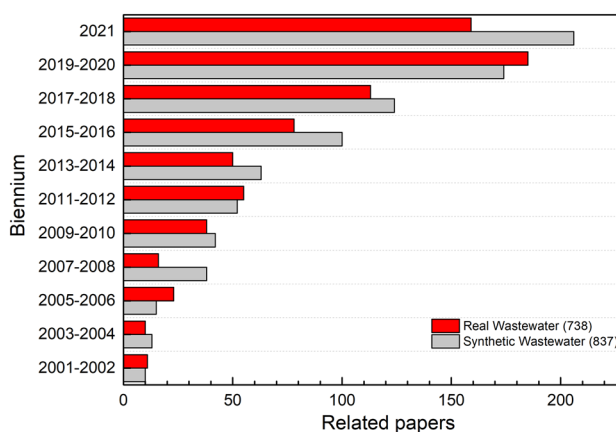


Fig. 1 Application of EAOPs in the electro-degradation of azo-dyes present in effluents. *Keywords:* Azo-dyes, removal, EAOPs, electro-coagulation, Electro*. Researched June 02, 22. Database: Web of science

shape of the electrochemical cell, the pH of the medium, the current density ($A\ m^{-2}$), supporting electrolyte, and the flow velocity (*e.g.* in cases of using flow systems for the process) (Siedlecka et al. 2018).

The importance of developing azo-dyes removal methods can be reflected in the significant increase in scientific research on the subject. As an example, Fig. 1 shows the variation in the number of publications over the last 20 years, where it is possible to verify an exponential increase in the use of advanced electro-oxidative processes for the degradation of azo-dyes present in both synthetic and real effluents. In this sense, an adjustment of bibliometric data to a generic exponential function allowed listing coefficients of determination of $R^2 = 0.9744$ and $R^2 = 0.9372$ for synthetic and real effluents, respectively. Another important observation is the analysis of the growth in the number of publications between the first two years with 2021. It was found that the number of works associated with synthetic effluents increased about 20.6 times and those of real effluents showed an increase of approximately 15 times about the 2001–2002 biennium.

From the bibliometric search, it was evident that the number of publications related to the use of EAOPs for the degradation of azo-dyes showed and still shows an increasing trend. It is noticed that the application of synthetic effluents in the removal tests is prominent when compared to real effluents. One of the reasons for this behavior is justified by the ease of compositional control of the solution under study, since real effluents have a huge variety of spectator chemical species (*e.g.*, metals, anions, and residual organics) that, in an electrochemical test, can damage the working electrode (*i.e.*, poisoning of catalysts) and make the execution of the method unfeasible (Waghmode et al. 2011).

Another reason is related to scaling up. Electrochemical tests involving only the species of interest (azo-dye) are essential to establish initial parameters of efficiency and subsequently increase to studies on an industrial scale, with real effluents and flow systems (Vaghela et al. 2005). However, although the use of synthetic effluent degradation studies via electrochemical techniques has some advantages, it is limited to defining the complexity of real procedures. This characteristic is more prominent when taking into account some parameters, such as Total Organic Carbon (TOC) and COD, which vary widely between a synthetic and real sample. Thus, an *in vitro* test with a synthetic sample may not always reflect, in fact, the reality of a purification treatment process.

As stated, EAOPs are powerful technologies for the degradation of environmentally harmful species. Thus, this work will provide a review of the aforementioned techniques, especially EO, aiming to better understand their effectiveness in purifying effluents rich in azo-dyes. In addition, this work will present an updated approach to what has been published more in the field of purification of effluents by electrochemical means. Thus, this proposal will have great potential to provide different conceptions that inspire research and better orient them to the topic reported. Therefore, this review aims to suggest new paradigms involving the application of EAOPs in different dimensions, from pilot-scale tests to large-scale industrial processes.

Azo-dyes and textile dyeing effluents

Some species, when exposed to electromagnetic radiation in the visible spectral region (400–700 nm), start to absorb it and appear colored. Species with this property are most often known as dyes and pigments. Chemically, dyes have chromophore groups in their structure, made up of conjugated unsaturated systems (CUS). Some autochrome groups are also present, which intensify the visual effect of the color due to the presence of acceptor or electron donor groups (Baban et al. 2003; Sudha et al. 2014). Among the best-known chromophore groups are $-C=C-$, $-C=N-$, $-C=O-$, $-N=N-$, and $-NO_2$ which change their color due to the synergistic process of resonance of the CUS (Pandey et al. 2007; Singh et al. 2019).

Synthetic dyes are mostly derived from petroleum or minerals and are classified according to the mode of application. In textile industries, dyes can be classified into azo-dyes, direct-dyes, disperse-dyes, sulfur-dyes, pigments, reactive-dyes, anthraquinone, and metal complex dyes (Gung and Taylor 2004). Among the listed classes, azo-dyes are one of the oldest and most common in the industry, used in the dyeing of various materials. These species have a wide spectral range of colors (around 420 nm to 699 nm), and therefore

represent about 65% of commercially available dyes (Coura et al. 2020). According to Ramsay and Nguyen (2002), azo-dyes are characterized by the presence of one or more azo groups ($-N=N-$), in addition to the presence of reactive vinyl sulfone groups ($RS(=O)(=O)-R'$), and the bonds between two or more aromatic rings, which ensure high stability for the structure due to resonance phenomena (Ramsay and Nguyen 2002; Vasconcelos et al. 2016). Furthermore, azo groups can also be linked to naphthalene structures, heterocyclics, or aliphatic groups (Bafana et al. 2011).

In technological research and development, some species of azo-dyes have been successfully applied to the operation of equipment such as lasers, 3D printers, LCDs, and photoelectric devices (Ibrahim et al. 1991). It is estimated that there are about 3000 different types of azo-dyes being produced and applied by industries today. Most azo-dyes used in the dyeing process are mono-sizes that have at least one chromophore group ($-N=N-$) which are normally linked by two aromatic systems (Girrane et al. 2008; Selvaraj et al. 2020). Some molecules composed of heterocyclics are applied for medicinal and therapeutic purposes, such as Violet acid and Yellow aniline.

Azo-dyes, when present in an aqueous medium, tend to undergo chemical and biological degradation, exacerbating the consumption of oxygen in the medium. Consequently, this behavior promotes alterations in the pH value of the industrial effluent (about two to three pH units, ranging from 5.9 to 8.9); reduction of dissolved oxygen (DO) (generally DO levels below 3 mg per liter ($mg L^{-1}$) are of concern, and waters with levels below $1 mg L^{-1}$ are considered hypoxic), variation in chemical and biological oxygen demands (COD and BOD) and finally alterations in the ionic balance of the aqueous body (Eden 1996).

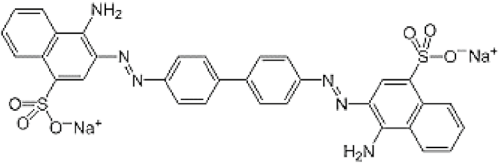
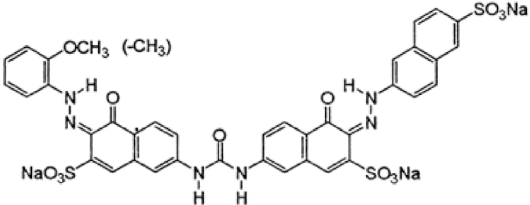
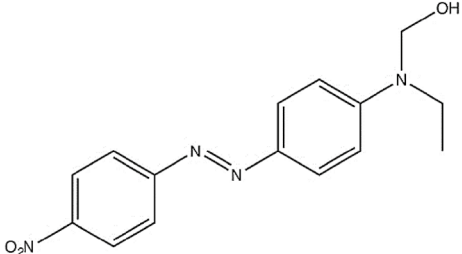
Specifically, azo-dyes are responsible for interfering with a range of biological processes, such as inhibition of DNA, RNA, protein synthesis dysfunction, reduced oxidant scavenging, reduced nitrogen metabolism, and genomic mutations (Catino and Farris 1985; Beharry and Woolley 2011). The degree of toxicity of azo-dyes defined by the European Union means that the lethal dose, which affects 50% of the tested species (LD_{50}), varies between 250 and 2000 $mg kg^{-1}$ of body mass (Clarke and Anliker 1980). Thus, some azo-dyes, such as Congo red, can have catastrophic effects on the human body. This species acts to inhibit the metabolism of serum albumin, aggregating to it and forming a structure of low solubility, which precipitates on connective tissues. Table 1 presents the main representatives of the family of azo-dyes used in the transformation industries, their structure, and hazardous effects.

Textile industries can be ranked as one of the most harmful to the environment, and large volumes of liquid effluents contaminated with dyes originate annually (around). Approximately 7×10^5 tons of dyes are produced annually,

Table 1 Some azo-dyes and their hazardous effect

Dye	Structure	CAS Number	Hazardous effect
Acid violet 7		4321-69-1	Acid violet 7 can induce the formation of chromosomal aberrations, lipid peroxidation, and degenerative effects (Bafana et al. 2011)
Reactive Orange 16		20262-58-2	Studies have been reported that this textile dye has a high mutagenic and teratogenic potential (da Costa Soares et al. 2017).
Reactive Red 228		140876-11-5	It has a high bioaccumulative and biomagnifying power, and can cause blindness in concentrations above its LD ₅₀ (da Costa Soares et al. 2017).
Aniline Yellow		60-11-7	Exaggerated exposure to this azo-dye caused malignant tumors in the urinary tract of tested mice (Puvaneswari et al. 2006).
Reactive black 5		17095-24-8	It restricts the efficient use of nitrogen by plants, reduces urease activity, in addition to being mutagenic and carcinogenic (Zhang et al. 2013).

Table 1 (continued)

Dye	Structure	CAS Number	Hazardous effect
Congo Red		573-58-0	It inhibits the functioning of serum albumin, aggregating to it and forming a structure of low solubility which precipitates on connective tissues (Pandey et al. 2007; Zhang et al. 2013; Singh et al. 2019).
Direct Red		2610-10-8	It causes mutagenic, carcinogenic effects, chromosome breakage, and respiratory intoxication (Khehra et al. 2005).
Disperse red 1		2872-52-8	It affects the intestinal flora, causing acute diarrhea and loss of cellular ionic balance. In large amounts, it can cause cancer of the gastrointestinal tract (Padmavathy et al. 2003).

of which 2.8×10^5 tons are not used and incorporate water-courses, causing devastating effects on the natural environment. This means that around 40% of the annual production is converted into effluent. Generally, effluents from textile industries present a chemical oxygen demand in a range of approximately 250 to 1900 mg L⁻¹ of O₂ (Huang et al. 2018). On the other hand, European environmental legislation estimates that for a textile liquid effluent to be released within the biosafety protocols, it must present a maximum COD value between 50 mg L⁻¹ to 20 mg L⁻¹ (Scalbi et al. 2005).

In general, textile effluents present relative conductivity, due to the presence of ions (e.g., sulfates and carbonates) from reagents used in the fabric processing steps. This characteristic favors the electrochemical oxidation process, not requiring the addition of salts to the medium that would act as supporting electrolytes. Furthermore, chloride ions may be present in the aqueous medium, favoring the generation

of active chlorine species with reactive oxygen species to mediate complete electrochemical oxidation. However, it should be considered that the efficiency parameters of the electro-oxidation process (COD, DOC, or color removal) have kinetics that are strongly dependent on the initial concentration of chlorine present in the effluents (Araújo et al. 2016).

In the literature, some authors such as Araújo et al. (2016) verified in their work that the use of dimensionally stable anodes (DSA) type for electro-oxidation of real textile effluents presented a decolorization of 85% in a time of 180 min, however, an addition of 0.5% (w/V) of NaCl to the effluent guaranteed the same effect in a time of just 100 min (Araújo et al. 2016; Keshavayya et al. 2018). This proves that the nature of the ions present in effluents is a factor intrinsically linked to the electrochemical efficiency of the oxidative process. Also, in the degradation efficiency segment, the decolorization index is considered one of the essential parameters

for the evaluation of the electrochemical process, since the main environmental standards, are based on the accentuated presence of coloration in the effluents.

Given the problems generated by the production and emission of textile effluents, it is necessary that engineering solutions such as, example, dimensioning, technical feasibility, and costs are optimized aiming at a better use of the water used in textile processing. Also, if the water treated via EO is reused in a new dyeing process, there will be a reduction of around 60% in the consumption of electrolytes and 70% in the volume of water (Sala and Gutiérrez-Bouzán 2014). Therefore, the electrochemical treatment prior to reuse promotes a clean chemical process with the high efficiency and low energy consumption possible. Furthermore, these mechanisms can promote processes reasonably eco-friendly.

Azo-dyes have been frequently degraded using physicochemical or biological techniques, which favor the discoloration of liquid effluents and reduce the toxicity of the product (Bafana et al. 2011). In general, each technique has its own advantages and limitations that depend on several factors, such as: the type of dye, composition and concentration of the effluent, hazardousness, cost-effectiveness, operational cost of large-scale implementation and intermediates formed during the process of degradation (Soni et al. 2020). The Fig. 2 presents a flowchart of the main technologies currently applied for the degradation of azo-dyes.

Different electrochemical techniques applied for the removal of azo-dyes

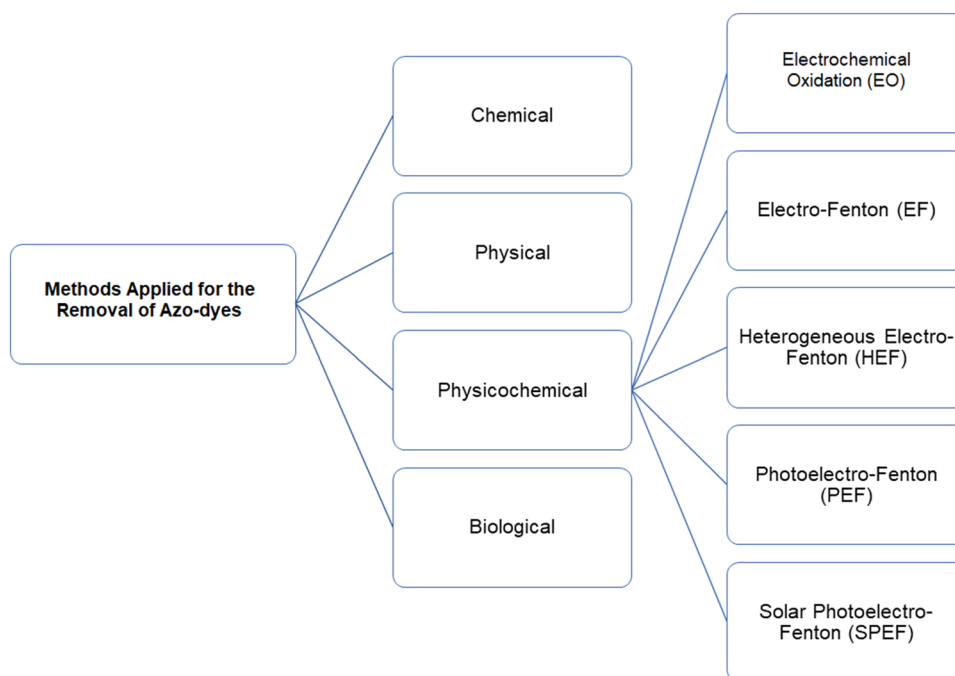
In the last 10 years, electrochemical processes have gained prominence in the remeasurement of liquid effluents containing azo-dyes. Thus, the most used and best performing electrochemical techniques for this purpose can be listed as those based on EAOPs (Khehra et al. 2005; Blanco et al. 2014). These electrochemical techniques are eco-friendly and have several advantages, for example, simplicity of equipment, relative easy operation, low operating temperature, can be easily combined with other technologies to enhance the degradation effect (Chekir et al. 2016).

Specifically, EAOPs have gained increasing attention in the context of purification of various effluents, such as those from the pharmaceutical, pesticides, azo-dyes, carboxylic acids and dioxins industries (Garcia-Segura and Brillas 2016). Among the different EAOPs, electrochemical oxidation (EO) is the most studied technique due to its enormous versatility and ease of application in different scales.

Electrochemical oxidation (EO)

In general, electrochemical processes involve oxidative reactions in the anode region, and reductive reactions in the cathode region. Based on this, such processes are supported by the fundamental idea that a redox reaction must occur in both compartments (*i.e.*, oxidation of persistent organics in the anode or reduction of heavy metals in the cathode), so that it is possible to guarantee the purification of the aqueous medium both in processes of reduction and electro-oxidation

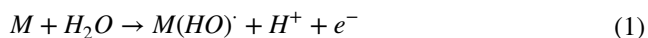
Fig. 2 Different techniques used in the degradation/removal of azo-dyes present in textile effluents



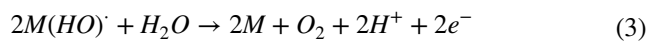
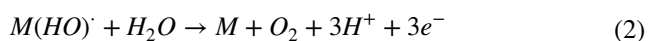
(Michael-Kordatou et al. 2015; Nancharaiah et al. 2015). The main characteristic that keeps the application of technologies based on electro-oxidation lies in the possibility of partially degrading or completely mineralizing persistent organic pollutants (POPs). Thus, the electrocatalytic properties of the materials used in anodes play a fundamental role in the electrochemical procedure (Sirés et al. 2014; Brillas and Martínez-Huitle 2015; Nancharaiah et al. 2015; Titchou et al. 2021a).

The electrochemical oxidation of POPs in an electrolytic cell can occur via two different mechanisms, which can be stated as (i) direct electrochemical oxidation and (ii) indirect electrochemical oxidation. Direct oxidation or simply electrolysis takes place directly on the anode surface and presents a net transfer of charges between the electrode and the POPs. The mechanism only involves the mediation of electrons that have the ability to oxidize some organic pollutants, under conditions of potentials less positive than the oxygen evolution potential (Soni and Ruparelia 2013). The direct oxidative process often requires adsorptive phenomena to occur on the anode surface. This process is defined as the limiting step and does not lead to general combustion of organic pollutants (García-Segura et al. 2018). Thus, when electrolysis is conducted under potential conditions lower than the oxidation potential of water, the electrodes become susceptible to surface poisoning, inhibiting the electrochemical oxidation process (Michael-Kordatou et al. 2015; García-Segura et al. 2018). On the other hand, in the indirect mechanism, the oxidation of the molecule of interest occurs through the formation of oxidizing agents, known as mediators, which are responsible for oxidizing the molecule of interest (Pelinson 2017; Soni et al. 2020). Different oxidizing species can be produced during EO, such as reactive oxygen species and active chlorine (Sandoval et al. 2019).

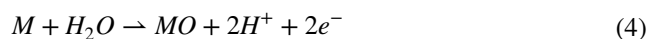
The indirect electro-oxidation process with reactive oxygen species is based on the electro-generation of adsorbed hydroxyl radicals (at a potential of 2.8 V/SHE) on the anode surface as an intermediate species of the oxygen evolution reaction (OER) (Cavalcanti et al. 2013). Thus, the initial reaction of the electro-oxidative process occurs through the formation of hydroxyl radicals adsorbed on the surface of the anodic electrode, Eq. (1).



In this case, M is designated as the anode and $M(HO)\cdot$ corresponds to the adsorbed hydroxyl radical. However, competitive reactions, such as those represented by Eqs. (2) and (3), can occur and consume the radicals to form oxygen in the evolution reaction, as can be seen,



Aiming to produce hydroxyl radicals in large proportion, anodes able to undergo overpotential above OER reaction should be used for ensuring the progress of reaction (1) with no parallel reactions (2 and 3) (Ribeiro and de Andrade 2006; Cañizares et al. 2006). According to Comninellis and Vercesi (1991), Comninellis and Pulgarin (1993), the electrocatalytic influence of anode materials is directly linked to the classification of the anodes used in overpotential conditions for OER. It appears, therefore, that electrodes can be classified into two types: “active” and “non-active” electrodes (Comninellis and Vercesi 1991; Comninellis and Pulgarin 1993). The different efficiencies verified in these electrodes, during the treatment of textile effluents, occur through the difference in enthalpies of the adsorption process on their surface. In general, species that undergo physisorption are considered to be better oxidants than species that are strongly attached to the surface (chemisorbed). Reaction (4) shows a chemisorption process on the electrode surface,



Specifically, active electrodes are only capable of performing a milder electrochemical conversion, transforming organic molecules into more biodegradable species, such as short-chain organics. These anodes cannot completely mineralize the pollutant or degrade them to the final CO_2 stage (Cavalcanti et al. 2013). This behavior can be explained by the high oxidation states of the metal or the metallic oxides used in the manufacture of electrodes, which have a standard potential above that required for the formation of OER ($E^\circ = 1.23$ V/SHE), leading to the preferential occurrence of desorbed active oxygen species on the electrode surface. As seen, the electrochemical efficiency of processes governed by chemical adsorption is lower compared to physical adsorption. Among the active electrodes, the most commonly reported in the literature are dimensionally stable anodes (DSAs), composed by TiO_2 , RuO_2 and IrO_2 (Martínez-Huitle and Ferro 2006).

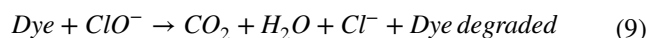
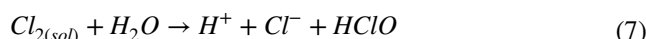
On the other hand, in non-active anodes, the hydroxyl radicals generated in reaction (1) undergo a physisorption process on the electrode surface. Subsequently, the radicals start to present greater mobility, reactivity, high oxidizing power to conduct electrochemical combustion processes of organic molecules. This degrades the pollutant to a minimal stage, *i.e.* complete conversion of POPs to CO_2 and water (Gargouri et al. 2014). Among the different types of materials used in non-active anodes, there are titanium dioxide (IV), ruthenium oxides (IV), lead oxides (IV), antimony oxides (IV) and boron-doped diamond electrodes (BDD) (Comninellis and Pulgarin 1993; Sandoval et al. 2019;

Titchou et al. 2021a). However, it is worth emphasizing that anode materials are not exclusively active or non-active, because in many cases they present ambiguous behavior, sometimes with active characteristics and sometimes with non-active characteristics.

A pertinent example is the BDD electrode, which has a maximum potential as a non-active anode. However, recent researches verified that this electrode has a dualistic characteristic, dependent on the structural conformation of the sp^2/sp^3 carbons, which have a high potential to affect its non-active behavior. In addition, BDD electrodes have different characteristics also due to the type of electrode activation, doping level and electrochemical activation. Specifically, the advantage of using BDD in these cases lies in (i) the largest electrochemical potential window for aqueous (~ 3.0 V– 3.5 V) and non-aqueous media (~ 5.0 V– 7.5 V); (ii) A small and stable background current, which is attributed to the low capacitance of the BDD material ($C = 10 \mu\text{F cm}^{-2}$) when compared with other materials, such as Au ($C = 30 \mu\text{F cm}^{-2}$); (iii) A broad electromagnetic transparency window ranging from the UV–Vis region to the far-infrared region; (iv) Electrochemical properties tunable by the boron concentration in the diamond lattice (Muzyka et al. 2019). Figure 3 shows the different mechanisms involved in the electro-oxidative process using active and non-active anodes.

Another type of indirect electro-oxidation process that deserves attention is the one mediated by chloroactive species. This technique is often applied for the purpose of removing highly toxic species (Garcia-Segura and Brillas 2016). The

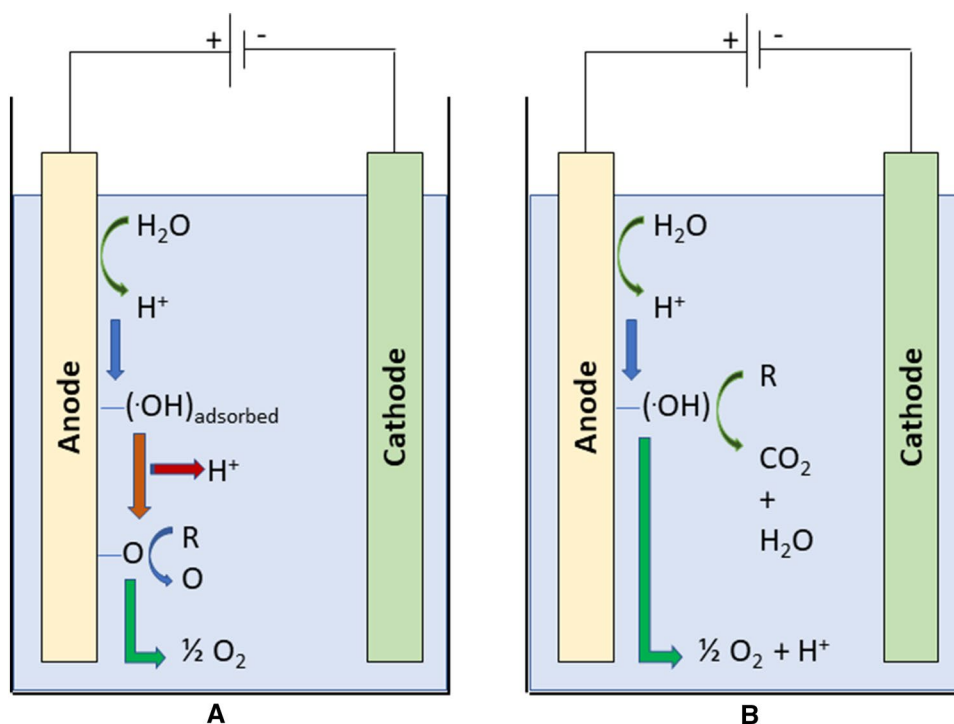
articles written by Rajkumar and Kim (2006); Martinez-Huitle and Ferro (2006) show the high efficiency of the EO process in electro-oxidation tests of dyes and pigments in textile effluents. Soni et al. (2020), Cañizares et al. (2006) showed that the reactions from (5) to (9) are those involved in the indirect process of electro-oxidation of azo-dyes involving electro-generation of active chlorine (Rajkumar and Kim 2006; Cañizares et al. 2006; Ferro et al. 2014; Michael-Kordatou et al. 2015; Soni et al. 2020).



According to Cañizares et al. (2006), the reduction of water in the cathode electrode will occur first, which will produce hydroxyl ions in the medium (5) (Cañizares et al. 2006). On the other hand, at the anode, the electro-generation of active chlorine will effectively take place (6).

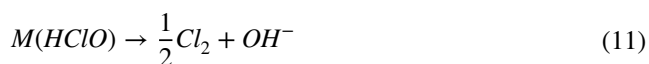
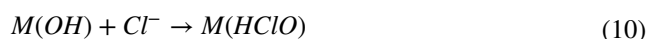
Under acidic pH conditions, the molecular chlorine present within the solution will form hypochlorous acid, as shown in Eq. (7), which is a potent oxidizing agent and is

Fig. 3 Scheme of action of **a** active and **b** non-active anodes in the electro-oxidation of pollutants using active oxygen species generated in situ. Reprinted (adapted) from Garcia-Segura et al. (2018), Copyright (2018), with permission from Elsevier



also responsible for stabilizing the pH of the medium in the range of 3.0–8.0. A high consumption of H^+ ions will increase the number of OH^- radicals within the solution, also increasing the pH and concentration of $HClO$. In this way, hypochlorous acid will act as a strong oxidizing agent, as mentioned, breaking the azo bonds. This break will promote a change in the chromophore structure of the dye, reducing the color of the solution (Cañizares et al. 2006).

Under other conditions, alkaline or neutral, $HClO$ depletion follows in accordance with Eq. (8). Under these circumstances, hypochlorite ions will form, which also function as excellent oxidants, acting readily in breaking the azo bond of the chromophore portion. The product of this mechanism will be Eq. (9), presenting, as a result, the degradation products of the dye, chloride ions, carbon dioxide and water (Duan et al. 2015). The dependence of pH on the oxidative efficiency of this active chlorine electrogeneration process is a crucial factor and must be considered. Thus, the standard reduction potential of Cl_2 ($E^\circ = 1.36$ V/SHE) and $HClO$ ($E^\circ = 1.49$ V/SHE) are considerably greater than ClO^- ($E^\circ = 0.89$ V/SHE). This indicates that the oxidative process of organic species will occur more efficiently and completely when it is carried out under acidic pH conditions. The possibility of simultaneous electrogeneration of chlorine-active species with oxygenated species was verified in works such as Bonfatti and contributors (2000), and Rosestolato et al. (2014). In this mechanism, oxygen transfer reactions will be carried out by oxy-chlorinated species and adsorbed by the reaction (10) as intermediates in the evolution of chlorine present in the reaction (11) (Bonfatti et al. 2000; Ferro et al. 2014; Rosestolato et al. 2014)



Regarding the industrial application of this technique, in recent years there has been a great increase in the use of chlorine electro-generation for purification processes of effluents from the most diverse fields. However, even though it is fast and efficient, when compared to the generation of adsorbed hydroxyl radicals, this technique can have some disadvantages, such as the formation of highly toxic organochlorine intermediates such, for example, haloacetic acids and halomethanes, in addition to persistent ionic species (Rosestolato et al. 2014; Radjenovic and Sedlak 2015).

In general, the materials commonly used in the manufacture of anodes used in electro-oxidation by chlorine-active are similar to those already described in this section. However, it is notable that the materials used in active anodes have better performance than non-active ones. Thus, it appears that the best electrocatalytic properties for chlorine

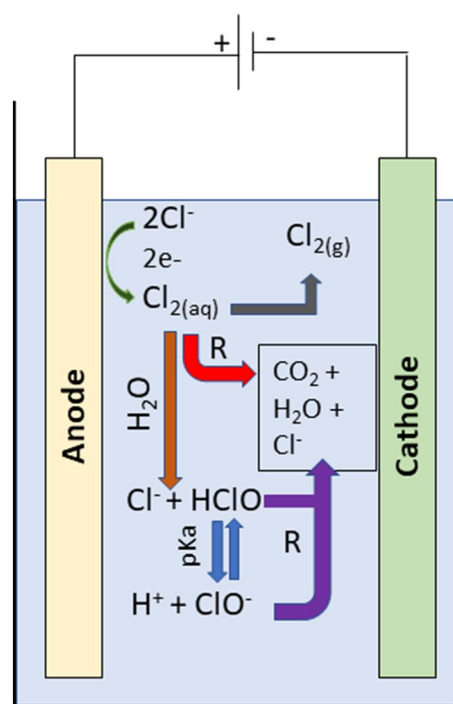


Fig. 4 Scheme of generation of active chlorine species for electro-oxidation processes of organic pollutants. Reprinted (adapted) from Garcia-Segura et al. (2018), Copyright (2018), with permission from Elsevier

evolution are found in active electrodes (*e.g.*, Pt, RuO_2 e IrO_2), which can effectively convert chloride ions to active chlorine (Bonfatti et al. 2000; Ferro et al. 2014; Rosestolato et al. 2014; Garcia-Segura et al. 2018).

Studies previously reported in the literature suggest that it is extremely necessary to stipulate minimum concentrations of active chlorine for the oxidation process to occur efficiently, but with a much smaller load of intermediates and within the limits required by environmental agencies. In fact, defining parameters and concentrations of application of chloro-active species on an industrial scale is a great challenge nowadays (Radjenovic and Sedlak 2015). Figure 4 presents a schematic of the electro-generation process of chlorine-active species acting on the indirect oxidation of organic pollutants.

Although active-chlorine and oxygenated species are the most used in indirect electro-oxidation processes, others also present in the solution can be selected to carry out pollutant oxidation processes, acting as mediators. These species are generated electrochemically from the oxidation of components of the electrolyte used, for example, sulfates, phosphates and hydrogen-carbonates yielding perosulfates, peroxydiphosphates and peroxydicarbonates (Peña 2017; Araújo et al. 2018). However, in comparative terms, these

oxidants are not capable of carrying out a complete oxidation of pollutants to the point of mineralizing them.

Dimensionally stable anodes (DSA)

Taking into account the main mechanisms of the EO process, direct and indirect, it is necessary to have a better understanding of the working electrodes, which are routinely applied to promote them. Therefore, Dimensionally Stable Anodes (DSA) can be considered as powerful working electrodes to promote the mineralization of persistent organic pollutants.

The DSA are composed of a metallic support, usually titanium (Ti), coated with electronically conductive or semi-conducting metallic oxides, such as RuO₂, PtO_x, TiO₂ and Ta₂O₅, which can present a high specific area due to their rough/porous surface (Vasconcellos et al. 2021; Gonzalez et al. 2016). DSAs also have excellent mechanical, electrical and electrocatalytic properties, and easy control of composition during the synthesis by combining mixtures of precursors. This enables a precise stoichiometric control in the manufacture of binary, ternary or quaternary metal oxide electrodes (Profeti et al. 2009). This combination of metals or metallic oxides is essential to raise the useful life of the material and improves the parameters of efficiency in the degradation process.

Beer (1963) introduced DSA electrodes in the 1960s, and for several decades, the use of these anodes was aimed at the chlorine-soda production. Although DSA have excellent properties for the electro-oxidation processes of organic molecules, their application in textile dye degradation is still a recent issue. In this context, one of the first works to be developed on DSA dates back to the 1970s, developed by Galizzioli and Trasatti (1973); and Galizzioli et al. (1975). The work function, electronegativity and electrochemical behavior of metallic oxides used in coatings on metallic supports were studied. However, it was only in the 1990s that DSA began to be widely used in the electro-oxidation of organic molecules, receiving due attention in the area of effluent treatment and macromolecule degradation (Boodts and Trasatti 1990). Currently, the availability of DSA is great, and the composition used in its preparation corroborates with the desirable properties of the final material.

The use of metal oxides in DSA aims to facilitate the transport of electrons for the target electrochemical reaction to take a place. Furthermore, the oxide layer promotes high chemical stability and favors catalytic activity. The development of an efficient electrode depends on the choice of its materials, mainly on the oxides used (Galizzioli and Trasatti 1973). As attested, the oxide to be chosen must present high conductivity and high stability, in order to reduce the electrode passivation and to guarantee a longer service life, respectively. Furthermore, the intense adhesion of the

mixture of oxides applied to the titanium metallic support is guaranteed by the formation of a thin layer of TiO₂ during the preparation heat treatments. Specifically, the different oxidation states of the cations present on the surface of the metallic oxide layer allow the adsorption of OH and O species, which can act as highly effective oxidizing agents in an electro-oxidation reaction. This feature consists of a strategy against the poisoning of the catalyst surface caused by the irreversible adsorption of fragments of organic molecules (Profeti et al. 2009).

DSA electrodes can be prepared using several methods, the most reported in the literature being the thermal decomposition of an appropriate precursor material (Steter et al. 2016; Soni et al. 2020). In general, oxide coatings are commonly prepared from salts of metal chlorides, dissolved in appropriate solvents, and subsequently applied to the metallic support of the electrode by brushing (Martinez-Huitile and Ferro 2006; Profeti et al. 2009; Baran et al. 2019; Soni et al. 2020). Regarding the effects of the procedure, the microstructural characteristics and the electrochemical efficiency of the metal oxide layer are largely influenced by the preparation method, the type of solution used, and the oxide synthesis temperatures (Soni and Ruparelia 2013). Some problems can arise from the synthesis of the electrode, for example, microstructural problems caused by brushing process in the preparation of the film layer or lost of metal ions by evaporation during the thermal treatment. Moreover, as the DSA preparation is a manual and artisanal procedure, the electrodes usually have reproducibility problems, which consequently causes variation in parameters during electrochemical tests (Sandoval et al. 2019; Titchou et al. 2021a).

In order to overcome this problem, the method of thermal decomposition of polymeric precursors instead inorganic salts precursors, is an alternative to ensure the stoichiometric compositions of the metals. In this procedure, resins are prepared, generally by heating a solution of the metal ions in ethylene glycol and citric acid, until finishes the polymerization process (Galizzioli et al. 1975). This resin containing the precursors is applied to the surface of the DSA support by brushing. In this method, precise control of stoichiometry is reached and the efficiency of the working electrode is ensured (Galizzioli and Trasatti 1973).

Considering the use of DSA toward the dye oxidation, Soni et al. (2020); Rajkumar and Kim (2006); Baddouh et al. (2018) studied the removal of dyes, and specially Reactive Black 5 and Rhodamine B, via indirect oxidation using active chlorine generated in situ. The studies demonstrated that the chemical oxygen demand of the real textile effluent reduced by around 75% and 89% when compared to the original COD. On the other hand, Titchou et al. (2021a, b) reported the efficient degradation of the azo-dye Acid Yellow 25 and Acid blue 29, showing reductions in COD from 78.0 to 89.5% using sodium chloride as electrolyte. Studies

Table 2 Application of titanium electrodes coated with multimetal oxides in the electro-oxidation of azo-dyes molecules present in real and synthetic effluents

Anode	Electrolyte	Azo-dye	Parameters	References
Ti/PtO _x -RuO ₂ -SnO ₂ -Sb ₂ O ₅	H ₂ SO ₄ /NaCl	Reactive black 5	$j = 5.00 \text{ mA cm}^{-2}$, COD: 85.0%, Decolorization: 99.6%	Soni et al. (2020)
Ti/TiO ₂ -RuO ₂	H ₂ SO ₄ /NaCl	Reactive black 5	$j = 15.00 \text{ mA cm}^{-2}$, COD: 75.0%, Decolorization: 79.0%	Rajkumar and Kim (2006)
Ti/ZrO ₂ -Y ₂ O ₃	NaCl	Acid blue 29	$j = 10.00 \text{ mA cm}^{-2}$, COD: 89.0%, Decolorization: 100%	Subba Rao and Venkatarangaiah (2014)
Ti/IrO ₂ -SnO ₂ -Sb ₂ O ₅	NaCl	Acid yellow 36	$j = 10.00 \text{ mA cm}^{-2}$, COD: 89.2%, Decolorization: 96.5%	Aguilar et al. (2018)
Ti/IrO ₂ -RuO ₂	H ₂ SO ₄ /NaSO ₄	Reactive black 5 oxamic dye 6	$j = 30.00 \text{ mA cm}^{-2}$, COD: 71.0%, 85.0% (respectively)	Vasconcelos et al. (2016)
Ti/TiO ₂ -RuO ₂ (DSA@-Cl ₂)	NaCl	Acid Yellow 25 Acid Blue 29	$j = 10.00 \text{ mA cm}^{-2}$, COD: 89.5%, Decolorization: 78.0%	Sandoval et al. (2019)
Ti/ SnO ₂ -IrO ₂ Ti/ RuO ₂ -IrO ₂	NaCl/Na ₂ SO ₄	Reactive black 5 direct red	$j = 10.00 \text{ mA cm}^{-2}$, COD: 92.4%, 88.2%, Decolorization: 89.0%, 90.1% (respectively)	Baddouh et al. (2018)
Ti/IrO ₂ -SnO ₂ -Sb ₂ O ₅	NaCl/Na ₂ SO ₄	Mixture of violet rl green a and brown DR	$j = 50.00 \text{ mA cm}^{-2}$, COD: 90.0%, Decolorization: ~85.0%	Bravo-Yumi et al. (2020)
Ti/TiO ₂ -RuO ₂ Ti/PtO _x -IrO ₂	NaCl/Na ₂ SO ₄	Blue 19 dye	$j = 50.00 \text{ mA cm}^{-2}$, COD: 81.4%, 92.0% (respectively)	Santos et al. (2020)
Ti/SnO ₂ -RuO ₂	Na ₂ SO ₄	Direct blue 86	$j = 20.00 \text{ mA cm}^{-2}$, COD: 78.3%–85.0%, Decolorization: 88.0%	Kumar and Gupta (2022)
Ti/SnO ₂ -Sb-CNT	Na ₂ SO ₄	Acid Red 73	$j = 50.00 \text{ mA cm}^{-2}$, COD: 80.0%, TOC: 60.0%	Isarain-Chávez et al. (2017)
Ti/TiO ₂ -RuO ₂ -IrO ₂	NaCl	Methyl red	$j = 20.00 \text{ mA cm}^{-2}$, COD: 90.0%, Decolorization: 99.9%, TOC: 77.2%	Sathishkumar et al. (2017)
Ti/TiO ₂ -RuO ₂	H ₂ SO ₄ /NaSO ₄	Mordant blue 13	$j = 100.00 \text{ mA cm}^{-2}$, COD: 98.0%, Decolorization: 100%	Kenova et al. (2018)
Ti/TiO ₂ -RuO ₂	NaSO ₄	Reactive blue 4	$j = 37.80 \text{ mA cm}^{-2}$, COD: 65.0%, Decolorization: 100%, TOC: 43.0%	Silva and Andrade (2015)
Ti/CoO _x -RuO ₂ -SnO ₂ -Sb ₂ O ₅	NaCl	Reactive black 5	$j = 50.00 \text{ mA cm}^{-2}$, COD: 26.5%, Decolorization: 97.0%, TOC: 25.0%	Saxena and Ruparelia (2019)
DSA ^a (De Nora) /BDD ^b	NaCl/Na ₂ SO ₄	Red reactive 5B	$j = 10.00 \text{ mA cm}^{-2}$, Decolorization: 63.0%	Cotillas et al. (2019); Titchou et al. (2021a, b)

^aDSA Dimensionally stable anodes

^bBDD Boron-doped diamond electrode

developed by Santos et al. (2020); Cotillas et al. (2019) and Titchou et al. (2021a, b) reported a reduction in COD values for Red Reactive 5B Dye and Reactive Blue 104 Dye from 58.0 to 63.0%, respectively. Table 2 shows some azo-dyes used in direct and indirect electrochemical oxidation tests promoted by active and non-active anodes (Santos et al. 2020).

Electro-fenton (EF)

The Electro-Fenton technique is considered an extension of the Fenton process, in which H₂O₂ is electrochemically generated in situ under acidic pH conditions. In general,

Fenton-based technologies are frequently reported to present high efficiency parameters in the removal of different pollutants (Brillas et al. 2009; Sennaoui et al. 2018; Babu et al. 2019). Some recent works, such as in Liu et al. (2021), show the importance and the most current developments in the generation of peroxide via Fenton and in other technologies based on Fenton. In Mousset et al. (2021) the importance of combining EF with biological treatments in order to enhance the removal effects was reported.

On the other hand, authors such as Steter et al. (2016) and Sirés et al. (2014) have carried out advanced studies of several trends for applications of EAOPs in the degradation of textile effluents, especially with the aim of updating

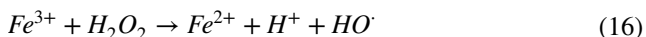
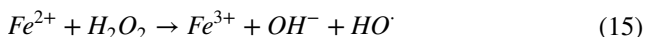
and circumventing the main limitations of the EF process. Among the various studies carried out, the works reported by Coha et al. (2021), Salazar-Banda et al. (2021) and Nidheesh et al. (2013) show that depending on the speciation of iron ions, the EF process can be represented in cathodic form or in anodic form. In the cathodic Fenton process, iron is added in its Fe(II) or Fe(III) salt speciation, and one or both Fe(II) and H_2O_2 reactants are produced in situ. On the other hand, in the anodic Fenton processes, also known as peroxicoagulation, the source of iron ions is the sacrifice of a metallic body made of Fe^0 (Brillas et al. 2009; Nidheesh 2018).

According to Titchou et al. (2021a, b) and Neyens et al. (2003) the processes involved in the original Fenton technique can be better described from Eqs. (15) to (23). Initially, we will have the reduction of gaseous oxygen at acidic pH, producing hydrogen peroxide. The Fe(III) ions present in the solution will be reduced to Fe(II) and the sacrificial metal body will be oxidized with regards to Fe(II) species forms. Reactions (12) to (14) present the processes (Neyens et al. 2003; Li et al. 2018).

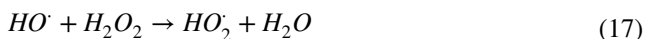


In view of the aforementioned reactions, which are considered of great importance for the formation of precursor reagents, reactions (15) to (20) present the initial stages, propagation and conclusion of the Fenton process.

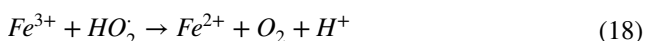
Start:



Propagation

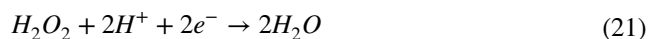


Finish:



According to Li et al. (2018) the removal process via EF has shown greater efficiency when the system operates under pH conditions around 3.0. Under pH conditions below 3.0 substantial reductions can occur in the presence

of equilibrium H_2O_2 according to reactions (21) and (22) (Adams et al. 2021). On the other hand, an enhanced and quick increase in the pH values can force hydrogen peroxide decomposition reactions in gaseous oxygen and water, in addition to decrease the solubility of iron ions in solution, producing a $Fe(OH)_2$ solid. Equations (21) to (23) describe the effect of pH on equilibrium displacement.



According to the main reactions of the EF process, some comparisons can be made between the latter and the traditional Fenton process. In general, the EF process has advantages such as, for example, the production of hydrogen peroxide in situ facilitates transport and makes the procedure safer. Moreover, the EF technique increases the oxidation rates of POPs and azo-dyes, since the regeneration of Fe^{2+} ions on the surface of the cathode electrode promotes a high efficiency of the oxidation process (Oturán and Aaron 2014). Another feature to be considered is the possibility of controlling and optimizing the degradation process and kinetics of electrochemical combustion, which enables the studies on mechanisms. Similar to the classic Fenton process, the EF process is related to the concentration of reagents used in the electrochemical procedure. Thus, an increase in Fe (II) and H_2O_2 concentrations could limit the process through cleaning reactions, in which a reduction in the reactivity of ($HO \cdot$) radicals occur. In general, EF processes can be implemented by combining this technique with electrochemical oxidation promoted by non-active anodes.

Yang et al. (2017) used graphite anodes to treat methyl orange via EF method. A color removal from the solution of about 98.6% was verified, with a current density (j) of 9 mA cm^{-2} in Na_2SO_4 medium (Yang et al. 2017). Rahmani et al. (2020) investigated the degradation of the azo-dye Acid Black 1 and Acid Blue 113 in batch assays with $j = 100 \text{ mA cm}^{-2}$, finding a color removal of 27.0% and 47.0%, respectively. Furthermore, a reduction in COD of 83.5% and 92.1%, respectively, were also verified (Rahmani et al. 2020).

Corona-Bautista et al. (2021) reported excellent results in the degradation of the azo-dye Brown HT, using a BDD electrode, in Na_2SO_4 medium and $j = 71 \text{ mA cm}^{-2}$, showing an efficiency of 100% in removing the color from the solution and 80% in reducing demand oxygen chemical. The degradation of the Basic Blue 9 dye was studied by Bustos-Terrones et al. (2021), using BDD with $j = 100 \text{ mA cm}^{-2}$ in Na_2SO_4 medium, with a removal of 97.7% in the wash bath coloration. On the other hand, da Costa Soares et al.

Table 3 Use of the EF technique with different electrodes to remove azo-dyes present in textile effluents

Electrode	Electrolyte	Azo-dye	Parameters	References
DSA ^a /BDD ^b	Na ₂ SO ₄	Methyl orange	$j = 9 \text{ mA cm}^{-2}$, COD: 75.6%. Decolorization: 98.6%. pH = 3.0	Yang et al. (2017)
BDD ^b	Na ₂ SO ₄	Acid black 1 acid blue 113	$j = 100 \text{ mA cm}^{-2}$, COD: 83.5% e 92.1%. Decoloriza- tion: 27%—47%. pH = 3.5	Rahmani et al. (2020)
BDD	Na ₂ SO ₄	Brown HT	$j = 71 \text{ mA cm}^{-2}$, COD: 80.0% e 92.1%. Decolorization: 100%. pH = 3.0 – 4.0	Corona-Bautista et al. (2021)
BDD	Na ₂ SO ₄ /H ₂ SO ₄	Basic blue 9	$j = 100 \text{ mA cm}^{-2}$. Decolori- zation: 97%. pH = 3.0	Bustos-Terrones et al. (2021)
Ti/TiO ₂ -SnO ₂ /BDD	Na ₂ SO ₄	Reactive orange 16 reactive violet 4 reactive red 228 Reactive black 5	$j = 35 \text{ mA cm}^{-2}$; COD: 75.6%. 81.0%. 69.3%. 75.0%. pH = 5.5	da Costa Soares et al. (2017)
BDD	NaCl	Brown HT eriochrome black	$j = 20 \text{ mA cm}^{-2}$. COD: 95.0% (Brown HT) and 91.0% (Eriochrome Black), Decolorization: 100% (both) pH = 2.8–3.0	Pacheco-Álvarez et al. (2019)
SS ^c -Graphite	Na ₂ SO ₄	Orange G	$j = 45 \text{ mA cm}^{-2}$. TOC: 20.0%, Decolorization: 75.00% pH = 3.0	Liu et al. (2019)
GDE ^d / nanoparticles of WO _{2.72} /BDD	K ₂ SO ₄ /H ₂ SO ₄	Orange II Sunset yellow FCF	$j = 50 \text{ mA cm}^{-2}$. TOC: 82.0% (Orange II)—90.0% (sunset yellow), Decolorization: 100% (both) pH = 3.0	Paz et al. (2019)
BDD/GDE	Na ₂ SO ₄	Acid red 1	$j \sim 67 \text{ mA cm}^{-2}$, Decoloriza- tion: 95.2% pH = 3.0	Wang (2022a)
CG ^e /SS	Na ₂ SO ₄	Methyl orange	$j = 80 \text{ mA cm}^{-2}$. TOC: ~45.0%, Decoloriza- tion: 94.5% pH = 3.0–4.0	Adachi et al. (2022)
CG/Pt	Na ₂ SO ₄ /H ₂ SO ₄	Mixture of industrial Azo- dyes	$j = 200 \text{ mA cm}^{-2}$. TOC: 65.0%, Decolorization: 93.0% pH = 3.0	Wakrim et al. (2022)
BDD/BDD	Na ₂ SO ₄	Blue BR brown mf violet SBL	$j = 18 \text{ mA cm}^{-2}$. TOC: Removal of 70.0%, 78.0%, and 82.0% for blue BR, violet SBL, and brown MF, decolorization: 60.0% (blue BR), 100% (Brown MF and Violet SBL), pH = 3.0	Alcocer et al. (2018)
BDD/GDE	Na ₂ SO ₄	Direct red 23	$j = 5.00 \text{ mA cm}^{-2}$. TOC: 98.0%, Decolorization: 100% pH = 3.0	Titchou et al. (2021a, b)
BDD/CF ^f	Na ₂ SO ₄	Naphthol blue black	$j = 30.00 \text{ mA cm}^{-2}$. TOC: 93.0%, Decolorization: 100% pH = 3.0	Afanga et al. (2021)
Iron	NaCl. KCl. Na ₂ SO ₄ . MgSO ₄	Acid red 18	$j = 1.0 \text{ A cm}^{-2}$. COD: 85.5%. 84.1%. 81.5%. 79.9%. pH = 3.0	Malakootian and Moridi (2019)

^aDSA Commercial dimensionally stable anodes^bBDD Boron-doped diamond^cSS Stainless steel electrode^dGDE Gas diffusion electrode^eCG: Carbon graphite electrode^fCF Carbon felt electrode

(2017) carried out more comprehensive studies on the effect of EF on azo-dyes, and found that the use of ADE of the Ti/TiO₂-SnO₂ type in medium at pH 3,0 and $j = 35 \text{ mA cm}^{-2}$, was able to effectively remove Reactive Orange 16, Reactive Violet 4, Reactive Red 228, Reactive Black 5 species (da Costa Soares et al. 2017). Table 3 presents these and other works reported in the literature that describe the application of FE to remove azo-dyes.

Heterogeneous Electro-Fenton (HEF)

The EF procedure proved to be very effective in the degradation of several pollutants, but each technique has its own advantages and limitations that will depend on several factors. Therefore, its application in acidic pH ends up restricting its execution on a large scale (Bello et al. 2019). The pH of industrial wastewater is commonly basic or neutral (Ganiyu et al. 2018), and under these conditions the solubility of iron ions in solution is decreased due to the formation of a precipitate of Fe(OH)_n. As a consequence, the decomposition of the generated H₂O₂ into water and O₂ hinders the production of radicals (HO·). In this case, it is possible that the electrocoagulation process is used to remove contaminants, instead of degradation (Nidheesh and Gandhimathi 2012). Therefore, the use of the heterogeneous electro-Fenton technique can be an ally to promote its application in the treatment of real effluents.

The development of HEF has aroused recent interest because it is a technique that allows waste treatment in a wide range of pH, using insoluble iron catalysts or cathodic materials with iron contents (Ganiyu et al. 2018). Although the kinetics of this technique is complex, the pH independence is achieved mainly by the production of the HO· radical through the heterogeneous Fenton reaction of the Fe²⁺ and H₂O₂, that will be controlled by the properties existing on the surface of the solid catalyst (represented by $\equiv Fe^{2+}$), as described in the reaction (24) (Brillas 2020).



where H₂O₂ is directly decomposed by Fe²⁺ catalyst into HO·, which can oxidize the pollutants until complete mineralization into CO₂ and H₂O. In addition, the iron-based catalysts can release small amounts of iron ions into the treated solution, which prevents the formation of sludge or iron sludge (Brillas 2021). These features increase efficiency and reduce process costs when compared to the conventional EF treatment since in the latter the iron catalyst is lost in the EF process because of the impossibility of separation from the treated effluent without a pH neutralization treatment that ensures environmental safety prior to disposal (Li et al. 2009). Another advantage of the HEF process is that

the solid catalyst may be recycled and reused after a careful cleaning of the surface, which is necessary in order to remove the organic by-products likely attached to it. These fragments of organic molecules strongly adsorb onto surface sites and inactivate them.

Furthermore, many materials can be designated as a model for the catalyst, which can be grouped into some categories, such as iron minerals, for example goethite and pyrite (Babuponnusami and Muthukumar 2013); iron supported materials, such as ion exchange resins and membranes, organic polymers and inorganic materials (Navalon et al. 2011); and iron nanoparticles (Dhakshinamoorthy et al. 2012). Functionalized materials, the so-called modified cathode materials, can also be used. In this case, the cathode performs a double function, both as a catalyst and an electrode, in order to guarantee a greater effectiveness of the reaction when considering the cathodic properties and electrical conductivity, in addition to the electrogeneration of H₂O₂ (Rosales et al. 2012; Poza-Nogueiras et al. 2018). These modifications can be metallic, made by carbon nanotubes and derivatives, airgel, bimetallic and non-metallic (Poza-Nogueiras et al. 2018).

Generally, many varieties of materials can be selected as model catalysts and a range of reaction conditions can be involved. Thus, it is essential to observe some criteria regarding the distinction of the catalyst for the success of the process. The catalytic materials must have a good catalytic activity in order to allow variations in pH and temperature. The chemical and mechanical stability are also important properties for ensuring that the catalysts can be reused (Ganiyu et al. 2018). The porous structure, large surface area and homogeneity are required for a good performance of the HEF catalysts (Poza-Nogueiras et al. 2018). In addition, the nature and amount of solid catalyst needed in the HEF must be taken into account, as well as the volume of treated solid and the organic matter content of the wastewater (Navalon et al. 2010).

Studies reported in the literature show that the HEF technique is efficient to catalyze the decomposition of H₂O₂ into HO· and, in turn, the mineralization of different classes of pollutants, especially POPs and azo-dyes. Jiang et al. (2016) reported excellent results for Methyl Orange degradation using RuO₂-Ti anode and a magnetite nanoparticle catalyst in Na₂SO₄ medium and current density (j) of 10 mA cm⁻², and obtained 86.6% removal of the dye from the aqueous solution. He et al. (2014a, b) carried out studies for the oxidation of the Methylene Blue dye in effluents using graphite anode assisted by a kaolin catalyst modified with Fe₂O₃ in NaCl medium applying $j = 69,23 \text{ mA cm}^{-2}$. In these conditions, it was obtained 100% efficiency in dye degradation and a removal of 96.47% of chemical oxygen demand

Table 4 Use of the HEF technique with different electrodes to remove azo-dyes present in dyeing effluents

Electrode	Electrolyte	Azo-dye	Parameters	References
RuO ₂ -Ti/ CB-PTFE ^a	Na ₂ SO ₄	Methyl orange	$j = 10.00 \text{ mA cm}^{-2}$, TOC: 32%, Decolorization: 86.6%, pH=3.00	Jiang et al. (2016)
graphite	NaCl	Methylene blue/methyl orange	$j = 69.23 \text{ mA cm}^{-2}$, COD: 96.5%, Decolorization: 100%, pH=3.00	Ma et al. (2009)
graphite	Na ₂ SO ₄	Methyl orange	$j = 68.00 \text{ mA}$, COD: 92.5%, Decolorization: 99.2%, pH=4.34	He et al. (2014a, b)
BDD ^b	Na ₂ SO ₄	Methylene blue	$j = 10.00 \text{ mA cm}^{-2}$, COD: 83.0%, Decolorization: 98.0%, pH=3.00	Zhao et al. (2016)
CoFe ₂ O ₄ /NOM magnetic hybrid catalyst	Na ₂ SO ₄	Acid black 210	$j = 45.40 \text{ mA cm}^{-2}$, COD: 95.0%, Decolorization: 100%, pH=6.00	Cruz et al. (2021)
Magnetite	Na ₂ SO ₄ /H ₂ SO ₄	C.I. Reactive blue 19	$j = 3.00 \text{ mA cm}^{-2}$, COD: 87.0%, Decolorization: 100%, pH=3.00	He et al. (2014b)
FeVO ₄ /CeO ₂ nanocomposites/ SS	Na ₂ SO ₄	Methyl orange	$j = 100 \text{ mA}$, COD: 70.0%, Decolorization: 96.3%, pH=3.00	Setayesh et al. (2020)
BDD/Carbon-PTFE	Na ₂ SO ₄	Acid blue 29 diazo	$j = 33.3 \text{ mA cm}^{-2}$, COD: ~45.0%, Decolorization: 100%, pH=7.00	dos Santos et al. (2019)
GE ^c /SS ^d	NaCl	Mixture of industrial azo-dyes	$j = 20.00 \text{ mA cm}^{-2}$, COD: 67.0%, TOC: 59.0%, Decolorization: 100%, pH=3.50	GilPavas and Correa-Sánchez (2019)
SS/GE	NaCl	Yellow 2G	$j = 12.50 \text{ mA cm}^{-2}$, TOC: 85.0%, Decolorization: 94.0%, pH=7.00	Benhadji and Ahmed (2020)
CoFe ₂ O ₄ /CF	Na ₂ SO ₄	Tartrazine dye	$j = 8.33 \text{ mA cm}^{-2}$, COD: 78.5%, Decolorization: ~100%, pH=3.50	Dung et al. (2022)
N-doped-CNF-Co/CoOx/CF	Na ₂ SO ₄	Acid orange 7	$j = 10.00 \text{ mA cm}^{-2}$, TOC: 92.4%, Decolorization: 100%, pH=3.00	Barhoum et al. (2021)
BDD/CF ^e	Na ₂ SO ₄	4-amino-3-hydroxy-2- p -tolylazo-naphthalene-1-sulfonic acid + Di-azo dyes	$j = 1.70\text{--}1.75 \text{ mA cm}^{-2}$, DOC: 95.0%, Decolorization: 90.0%, pH=2.9–4.0	Labiadh et al. (2015)

^aCB-PTFE: Carbon Black – Polytetrafluoroethylene Electrode

^bBDD Boron-doped diamond

^cGE Graphite electrodes

^dSS Stainless steel electrode

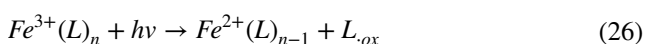
^eBDD/ CF Boron-doped diamond/Carbon felt

(COD). Table 4 shows some works reported in the literature that describe the application of HEF for the removal of azo-dyes.

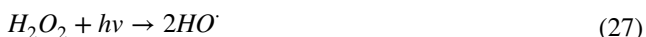
Photoelectro-Fenton (PEF) and Solar Photoelectron-Fenton (SPEF)

The association of irradiation with the conventional EF process will characterize the PEF and SPEF techniques, by artificial light or natural sunlight, respectively. Several strategies have been developed by research groups in order to minimize the problems arising from the oxidation processes

of organic pollutants. Homogeneous and heterogeneous PEF treatments, as well as SPEF, have been highlighted since these photo-assisted techniques have provided the increase in mineralization efficiency (Brillas 2020). This effect happens for two main reasons: (i) the competitive photoreduction reactions of Fe(III) complexes at pH values close to 2.8 to 3.5, with consequent production of $HO\cdot$ and regeneration of Fe(II) (Sun and Pignatello 1993); (ii) the direct photolysis caused by excitation of ligand–metal charge transfer of Fe(III)/organic intermediate compounds complexes, possibly formed in the process (Horváth and Stevenson 1993), such as carboxylic acids and weak oxidizing species. These processes will be described by reactions (25) and (26).



In the PEF method, the effluents are treated using artificial lamps with exposure in the UVA region at wavelength (λ) ranging from 315 to 400 nm, UVB at $\lambda=280$ –315 nm, and UVC at $\lambda < 280$ nm (Brillas 2014). Although UVA is the most used (Borràs et al. 2013), depending on the wavelength and intensity of the radiation source, pollutants can be degraded by different mechanisms. Direct photolysis of these components will occur when the light source emits radiation in the same length range in which these contaminants will absorb this radiation, that is, in the most efficient possible way. Furthermore, the application of UVC light in the presence of symmetrical peroxides such as H_2O_2 can lead to $HO\cdot$ additional formation through the homolytic cleavage of the peroxide bond, as showed in Eq. (27) (Khataee and Zarei 2011).



The application of light overcomes the limitation of the EF method in the presence of organochlorine compounds, for example, because different reactive species, such as $\bullet Cl_2$, $\bullet Cl$ and $\bullet HOCl^-$ can be generated in the medium (Coledam et al. 2018). However, monitoring of these products is necessary to avoid the production of toxic derivatives.

Aiming at the treatment of industrial effluents, the heterogeneous PEF processes have been investigated addressing the use of insoluble solid catalysts or cathodic materials iron-functionalized, similar to those described in 3.3. (Peng et al. 2015). The Fe solid catalyst or cathode ($\equiv Fe^{2+}$) immersed in the solution, is usually hydroxylated with $-OH$ groups, which can produce the same reactive oxygen species as the homogeneous PEF, to assume that similar reactions take place on its surface, according to Eq. (24). This promotes the formation of the radical $HO\cdot$ in basic or neutral pH in the presence of incident light, in addition to decreasing

the dissolution of Fe(III) ions, and ensuring the stability and reuse of the catalyst.

Despite the high efficiency of the PEF technique, the use of artificial lamps is commonly responsible for high electrical costs, which can be much higher than the cost of an electrochemical cell. This consumption can be minimized by applying the SPEF process, where the solution is directly irradiated with photons of natural sunlight, which is a free and renewable resource (Peng et al. 2015). The disadvantage of the method is that it restricts the daily hours of sun, the climate of the region, and its geographical location. However, if the input current is supplied by photovoltaic panels and stored in batteries, it can be an inexpensive power source for the electrochemical cells and UV lamps, in order to carry out a suitable hybrid treatment for an effective remediation content of dyes in effluents (Moreira et al. 2013; Brillas 2014, 2020).

Among the classes of synthetic dyes, azo-dyes are the most commercialized, around 70% of the total (Selvaraj et al. 2020). Several studies have demonstrated remarkable initial discoloration rates and dye removals, Solano et al. (2015) found 99% COD removals from the PEF-UVA process for Congo Red treatment using BDD anode at $j = 100 \text{ mA cm}^{-2}$. An improvement of the PEF process was performed by Iranifam et al. (2011a) by adding ZnO nanoparticles that allowed a mineralization of 94.7% of Basic Yellow 28 through a platinum anode at $j = 100 \text{ mA cm}^{-2}$. Moreira et al. (2017) found 93% DOC removals by SPEF for the treatment of Sunset Yellow FCF with BDD anode at $j = 100 \text{ mA cm}^{-2}$. Table 5 presents some studies of the degradation of different azo-dyes and description of the processes based on recent applications.

Evaluation of the feasibility of the process

During the electrolysis process, the efficiency in removing the color from effluents contaminated with dyes can be followed by determining the decay of the color intensity, using the Eq. (28).

$$(\%)CR = \frac{ABS_0 - ABS_t}{ABS_0} \times 100 \quad (28)$$

In this equation, the terms ABS_0 and ABS_t correspond to the maximum absorbance at a given visible wavelength, in the initial stages and at time t of the electrolysis process, respectively (Brillas et al. 2009). However, in the evaluation of the process by color removal ((%)CR), the incomplete dye oxidation and intermediates of oxidation reaction are not detected, since many of the species do not absorb radiation at the same wavelength as the chromophore portion of the dye. Furthermore, the (%)CR does not allow a

Table 5 Use of PEF or SPEF technique with different electrodes to remove azo-dyes present in textile effluents

Process	Electrode	Electrolyte	Azo-dye	Parameters	References
PEF-UVA	BDD/C-PTFE ^a	Na ₂ SO ₄	Congo red	$j = 100.00 \text{ mA cm}^{-2}$, COD: 99.0%, Decolorization: 100%, pH = 3.0	Solano et al. (2015)
PEF catalyzed by ZnO nanoparticles	Pt/CNT-PTFE ^b	Na ₂ SO ₄	Basic yellow 28	$j = 100.00 \text{ mA cm}^{-2}$, TOC: 94.7%, Decolorization: 91.3%, pH = 3.0	Iranifam et al. (2011b)
SPEF	BDD/C-PTFE ^a	Na ₂ SO ₄	Sunset yellow FCF	$j = 100.00 \text{ mA cm}^{-2}$, COD: 93.0%, Decolorization: 100%, pH = 3.0	Moreira et al. (2017)
PEF-UVA	BDD/C-PTFE ^a	Na ₂ SO ₄	Acid red 29	$j = 17.00\text{--}100.00 \text{ mA cm}^{-2}$, COD: 92.0%, Decolorization: 98.0%, pH = 2.0–6.0	Almeida et al. (2012)
SPEF	DSA/SS ^c	NaCl/ Na ₂ SO ₄	Acid red 1	$j = 15.00 \text{ mA cm}^{-2}$, COD: 75.0%, Decolorization: 100%, pH = 3.0	Murrieta et al. (2020)
PEF-UVC	BDD, MnO ₂ -ADE ^d	K ₂ SO ₄	Reactive black 5	$j = 50.00 \text{ mA cm}^{-2}$, TOC: 91.0%, Decolorization: 100%, pH = 3.0	Aveiro et al. (2018)
PEF-UVA	BDD/ADE	Na ₂ SO ₄	Orange G	$j = 200.00 \text{ mA cm}^{-2}$, TOC: 94.0%, Decolorization: 100%, pH = 3.0	Pereira et al. (2016)
SPEF	DSA ^e /ADE	Na ₂ SO ₄	Methyl orange	$j = 60.00 \text{ mA cm}^{-2}$, TOC: 98.0%, Decolorization: 100%, pH = 6.0	Salazar et al. (2022)
SPEF	DSA/ADE	Na ₂ SO ₄	Acid blue 29	$j = 25.00 \text{ and } 50.00 \text{ mA cm}^{-2}$, TOC: 75.0%, Decolorization: 100%, pH = 3.0	Salazar et al. (2019)
PEF catalyzed by FeS ₂ nanoparticles	BDD/CF	Na ₂ SO ₄	4-amino-3-hydroxy-2-ptolyazo-naphthalene-1-Sulfonic acid (AHPS) azo Dye	$j = 7.50 \text{ mA cm}^{-2}$, TOC: 95.0%, Decolorization: 100%, pH = 3.0 – 4.0	Labiadh et al. (2015)
PEF-UVA	BDD/SS	Na ₂ SO ₄	Chocolate brown HT eriochrome black	$j = 20.00\text{--}48.00 \text{ mA cm}^{-2}$, COD: 97.0%–99.9%, Decolorization: 100% (both), pH = 2.80–3.0	Pacheco-Álvarez et al. (2019)
PEF-UVA	BDD/CF	Na ₂ SO ₄	Acid red 1	$j = 33.40 \text{ mA cm}^{-2}$, COD: ~ 87.0%–99.9%, Decolorization: 96.7% pH = 3.0	Wang (2022)
PEF-UVC	Ti/PtO _x BC ^f -PTFE	Na ₂ SO ₄	Methyl orange	$j = 40.00 \text{ mA cm}^{-2}$, TOC: 80.0% Decolorization: 100.00% pH = 3.0	Kong et al. (2020)
PEF-UVA	DSA/CF-ADE	Na ₂ SO ₄	Methyl orange	$j = 20.00 \text{ mA cm}^{-2}$, TOC: ~ 94.0%, Decolorization: 100% pH = 3.0	Márquez et al. (2020)

^aBDD/C-PTFE Boron-doped diamond /carbon– polytetrafluoroethylene electrodes

^bPt/CNT-PTFE Platinum/carbon nanotube–polytetrafluoroethylene electrodes

^cSS Stainless steel electrode

^dADE Air diffusion electrode

^eDSA Dimensionally stable anode

^fBC Black carbon

quantitative analysis of the electro-oxidation performance, which makes it a useful technique for semi-quantitative analysis (Brillas et al. 2009; Nidheesh and Gandhimathi 2012). Another very useful analytical method for monitoring the electro-oxidation reaction is high performance liquid chromatography (HPLC). This technique allows the sensitive and quantitative identification of the products generated in the electrolysis reaction (Martínez-Huitle and Brillas 2009).

In addition to (%)CR and HPLC, other methods for monitoring the extent of the electrochemical reaction can be used. The total organic carbon content (TOC) and chemical oxygen demand (COD) are the most usual in stages of complete persistent organic pollutants (POP) mineralization. Equations (29) and (30) mathematically describe TOC and COD values.

$$TOC(\%) = \frac{TOC_0 - TOC_t}{TOC_0} \times 100 \quad (29)$$

$$COD(\%) = \frac{COD_0 - COD_t}{COD_0} \times 100 \quad (30)$$

In these equations, COD_t and TOC_t are the experimental values of chemical oxygen demand and experimental total organic carbon at time t (mg L^{-1}), on the other hand, COD_0 and TOC_0 are the initial values of COD and TOC. Additionally, other analyses of interest are the current efficiency (CE), which can be given from the variation of the COD during the experiment, as Eq. (31), and the measured current efficiency (MCE) for complete POP mineralization, obtained by Eq. (32).

$$CE(\%) = \frac{\Delta(COD)FV_s}{8It} * 100 \quad (31)$$

$$MCE(\%) = \frac{nFV_s\Delta TOC_{exp}}{4.32 \times 10^7 m.I.t} * 100 \quad (32)$$

wherein F corresponds to Faraday's constant ($9.6487 \times 10^4 \text{ C mol}^{-1}$), I is the electric current (A), V_s is the solution volume (L), 8 is the O_2 equivalent mass, $\Delta(COD)$ is the chemical oxygen demand decay, t is the time (s), $\Delta(TOC)_{exp}$ is the experimental change in TOC values at time t ; m and n are the number of carbon atoms and theoretical electron exchange during the mineralization process of organic compounds. The constant value (4.32×10^7) corresponds to the homogeneity correction factor. Under constant current conditions, an efficient electrolysis process guarantees low specific energy consumption values.

Cost analysis of the processes

The economic aspects are important issues in developing clean processes. So, developing affordable, energy-saving, and highly-effective technologies is extremely desirable as a way to increase access to sustainable production by different industrial sectors.

Despite their efficiency, electrochemical methods are frequently considered expensive, as they require energy to operate. Hence, energy consumption measurement is an important criterion in choosing the degradation method. Currently, the estimation of energy consumption per volume of treated effluent (E_{cons} , kWh m^{-3}) or the specific energy consumption based on COD removal (SEC, in $\text{kWh (kg (COD))}^{-1}$), are the values provided by the authors for comparison between technologies. Usually, electrode costs and sludge treatment are not considered in most studies. In the COD-based approach, the specific energy consumption (SEC) of the system is calculated by Eq. (33) (Ahmed Basha et al. 2010; Rahmani et al. 2015), whereas the energy consumption per volume (E_{cons}) is given by Eq. (34) (Azarian et al. 2018).

$$SEC = \frac{VIt}{\Delta CV_R} \quad (33)$$

$$E_{cons} = \frac{VIt}{v} \quad (34)$$

In the Eqs. (33) and (34), the V is the electric potential (V), I is the electric current (A), t is the reaction time (h), ΔC is the difference in inlet and outlet concentration of COD (g L^{-1}), and V_R and v are the volume of dye solution in L and m^3 , respectively.

The state-of-the-art of electrochemical oxidation processes shows an energy consumption ranging from 0.5 to 100 kWh kg COD^{-1} (Avlonitis et al. 2003; Xiao et al. 2015; Lee et al. 2016; Zou et al. 2016). Among the works which have estimated the energy consumption, Ozturk and Yilmaz (2020) showed the indirect electrooxidation of Basic Red 13 on Ti/Pt anodes. The energy consumption values of the system were calculated as 7.91 kWh m^{-3} and $0.98 \text{ kWh kg COD}^{-1}$ under optimal conditions to achieve high removal efficiency (99.98%), such as a current density of 19.53 mA cm^{-2} and pH 4.38. In another study, Morais et al. (2013) investigated the direct electrochemical oxidation of methyl red dye using Ti/Ru_{0.34}Ti_{0.66} electrodes. In this study, the energy consumption measured during galvanostatic electrolysis of dye solutions largely depended on the applied current density, and the authors found 11.03 kWh m^{-3} at 30 mA cm^{-2} (25°C). The electrochemical decolorization of methyl red by RuO₂-IrO₂-TiO₂ electrode through

hypochlorite formation was investigated by Sathishkumar et al. (2017). The authors calculated the cost of energy consumption for the decolorization of dye for 99.96% decolorization as 0.43 kWh m^{-3} . Li et al. (2017) developed a carbon nanotube filter for electrooxidation of methyl orange and others organic pollutants. In this work, the energy per volume of treated dye solution was calculated to be 0.19 kWh m^{-3} . Zhou et al. (2011) compared the electrochemical degradation of methyl orange on the mixed metal oxide (ruthenium-based DSA) and boron-doped diamond (BDD) electrode in the presence of NaCl. It was proved that the degradation on BDD electrode was better cost-effective and more suitable towards dye mineralization than metal oxide anode. On BDD, an energy requirement of 15 kWh m^{-3} could obtain a COD removal higher than 90% for an initial dye of 200 mg L^{-1} .

Another study, performed by Kumar and Gupta (2022), the electrochemical oxidation of direct blue 86 dye was investigated using an electrochemical system DSA-based ($\text{Ti/Sn}_{0.62}\text{Ru}_{0.38}\text{O}_2$), under four different current density conditions. In this investigation, a specific energy consumption of about 9.06 kWh m^{-3} at a current density of 20 mA cm^{-2} was observed. On the other hand, under conditions of low current density, a consumption of about 3.5 kWh m^{-3} was obtained. So, the specific energy consumption (SEC) increased significantly from 1.82 to 9.06 kWh m^{-3} with increase in current density. However, the reduction in electrolysis time and dye removal efficiency was not significant at high current densities. In addition, the authors investigated the mean operating cost for the procedure, which was estimated to be around $1.29 \text{ US\$ m}^{-3}$.

Alcocer et al. (2018) investigated the electrochemical degradation of the Violet Acid 90, Brown MF and Blue BR dyes, using a BDD-based electrode as anode at $j = 18 \text{ mA cm}^{-2}$. The authors obtained the specific average current consumption ranging from 23 to 33 kWh m^{-3} . In addition, decrease of the discoloration index and COD about 80% and 100%, for volume 0.5 L of treated effluent was described. Furthermore, the average operating cost was around $2.96 \text{ US\$ m}^{-3}$ to $4.50 \text{ US\$ m}^{-3}$, with considerable variations proportional to the current density applied during the procedure. Vasconcelos et al. (2019) investigated the electrochemical oxidation of the Reactive Blue 19 dye on an electrode based on Ni/BDD, with a specific energy consumption of 18.3 kWh m^{-3} of treated solution, under conditions of j : 41 mA cm^{-2} and 0.85 L of effluent. Furthermore, the reported efficiency parameters indicated a reduction of up to 70% in the absolute values of TOC.

Tang et al. (2020) conducted degradation studies of the azo textile dye X-6G employing an electrochemical system based on BDD, under j : 100 mA cm^{-2} and 0.01 mol L^{-1} of Na_2SO_4 as support electrolyte. In the investigations, it was found that after 2 h of electrolysis, the degree of

mineralization of the dye was high, and the rate of reduction of TOC presented values of 72.8%. In addition, the energy consumption required for dye degradation was 44.86 kWh m^{-3} , with an average operating cost of about $3.58 \text{ US\$ m}^{-3}$ for the treatment of 0.2 L of effluent. In another investigation, conducted by Elaissaoui et al. (2019), studies were carried out aiming at the degradation of Amaranth azo dye, using a system based on modified PbO_2 /Stainless Steel electrode, under j : 25 mA cm^{-2} . It was possible to verify an energy consumption of about 34.19 kWh m^{-3} for an effluent volume of 1L during 300 min of electrolysis. Del Río et al. (2009), investigated the use of an electrode based on $\text{Ti/SnO}_2\text{-Sb-Pt}$ under j : 125 mA cm^{-2} in $\text{NaCl } 0.05 \text{ mol L}^{-1}$ for the degradation of the dye C.I. Reactive Orange 4. In this work, COD removal efficiency of 94.2% was verified, accompanied by a specific energy consumption between 20.0 and 26.0 kWh m^{-3} , for a volume of 0.055 L and an initial concentration of 800 mg L^{-1} .

As stated, the current literature has an extensive approach to quantification, costing and optimization of EAOP-based techniques for the degradation of Azo dyes (Oturan and Aaron 2014). Brillas and Martínez-Huitle (2015) show that energy parameters related to specific consumption and operating costs are essential figures of merit for to evaluate the feasibility of electrochemical treatments of dyes for industrial application. Thus, in the approaches listed in this review, specific consumption values within the range of $\sim 1 \text{ kWh m}^{-3}$ – 40 kWh m^{-3} were verified, while the average energy costs reported ranged from $1.99 \text{ US\$ m}^{-3}$ to incomplete oxidation conditions, reaching the level of $10.52 \text{ US\$ m}^{-3}$ with the use of more energetically expensive systems based on BDD electrodes. Further in approaching the feasibility, cost and efficiency of EAOPs, the validation of the formed products, as well as the establishment of techniques aimed at monitoring become essential. Thus, knowing the main intermediaries and elucidating their mechanisms of formation and consumption is important, since allow us to predict the impact of the technique on the removal of the contaminant as a whole (Javaid and Qazi 2019).

Intermediates generated during the electrochemical procedure (by-products)

During the execution of the electrochemical method, it is extremely necessary to monitor intermediate reaction species, such as highly toxic organic molecules and inorganic ions. In general, this monitoring helps to determine the main degradation route and, consequently, the type of resulting effluent, in order to be able to categorize it within the legal emission standards. Specifically, analytical techniques such as high-performance liquid chromatography (HPLC) and gas chromatography coupled with a mass spectrometer (GC-MS) can identify the presence of different intermediate species

arising from the electro-oxidation process (e.g., organochlorines, carboxylic acids, inorganic ions and phenols) (Brillas et al. 2009; Moreira et al. 2017). Furthermore, the HPLC technique can be used to monitor the oxidation kinetics of POP (Oh et al. 2014; Solano et al. 2015; Zazou et al. 2019). Solano et al. (2015), Soni et al. (2020); and Rajkumar and Kim (2006) reported that the use of techniques such as HPLC in the identification of intermediates allowed the detection of approximately 13–15 hydroxylated derivatives, 21–35 aromatic intermediates, 6 phenolic derivatives and persistent inorganic ions. These data come from the analysis via HPLC of a sample of dyes: reactive black 5, congo red and acid violet that underwent the EO processes with DSA, EF and PEF, respectively. In all EAOPs mentioned, the formation of intermediates such as benzene, naphthalene, biphenyl, monoazo, diazo and phthalic acid was verified. Furthermore, tartaric, tartaric, oxamic, oxalic and acetic acids were detected in the analysis. In addition, the works reported that most of the nitrogen was lost during the process in the form of N-volatile species and oxidized to NO_3

and to a lesser extent to NH_3 (Oh et al. 2014; Solano et al. 2015; Çelebi et al. 2015; Zazou et al. 2019).

Scaling-up and pilot scale

The applicability of the electrochemical methods highlighted in the previous discussion strongly depends on the elucidation of projects for large-scale applications, for example, for the treatment of real effluents in flow cells. Valero et al. (2014) evaluated the feasibility of a treatment for removing pollutants from a real industrial effluent by electrochemical oxidation performed on a laboratory scale, and then its application on a pre-industrial scale. In the first stage, the work was carried out on a laboratory scale, using a 63 cm^2 cell, different anodes (Ti / Pt, and DSA (Ti / RuO_2 and Ti / IrO_2)), ideal experimental conditions (pH, current density, temperature), and chloride concentration (C_{Cl}) were studied and established. It was verified that a DSA- Cl_2 (Ti/ RuO_2), $\text{pH} = 9,0$, $j = 50 \text{ mA cm}^2$, $C_{\text{Cl}} = 2000 \text{ mg L}^{-1}$, and room temperature were the ideal conditions for the procedure in the laboratory. The chemical oxygen demand (COD) was reduced by up to 75%, indicating that the electro-oxidation process can satisfactorily remove organic pollutants. In the second stage, the process was scaled from laboratory to pre-industrial scale, using a 3300 cm^2 cell. The electrochemical reactor was then powered by a photovoltaic generator connected directly to it, in order to operate using renewable energy. The general procedure achieved a COD pollutant clearance of about 80% and a drastic reduction in TOC values to above 56% from the original values. The prototype used can be better presented in Fig. 5.

In the illustration proposed by Valero et al. (2014), it is possible to verify the detailed scheme for an application of the treatment process on a pre-larger scale, through a reactor. In (1) there is the Solar Photovoltaic generator; in (2) Electrochemical reactor; (3) Solution reservoir; (4) Thermometer and pH-meter; in (5) Flow rate meter; ((⊙)) corresponds to the system pump; ((⊗)) is the controlling valve, and ((■)) is the heat exchanger. When using the proposed system, it was verified that the COD elimination rate reached 70%, reduced to levels compatible with the discharge limit established by legislation. Thus, the feasibility of these systems is proven for pollutants present in real effluents. However, the studies developed by the authors did not show real evidence regarding the identification and quantification of by-products. This criterion becomes fundamental since the EO associated with DSA in chlorinated media (Cl^-/Cl_2) promote the formation of intermediate species of high toxicity (organochlorine), which were not classified by the methodologies used by the authors (Martínez-Huitle and Brillas 2009; Moreira et al. 2017; Sirés and Brillas 2021). Another point not investigated in the authors' scale-up proposal concerns the faradaic efficiency data of the process, nor the

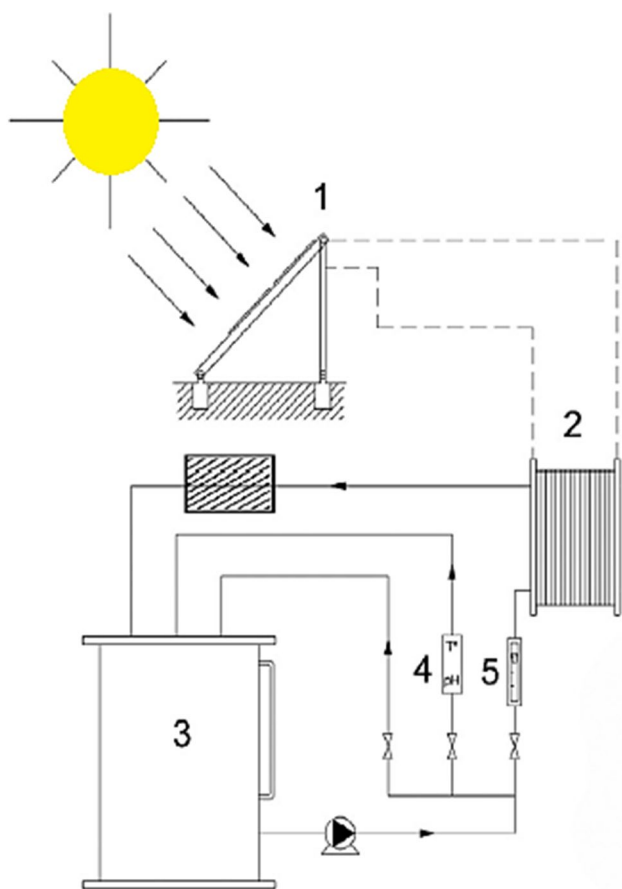


Fig. 5 Scheme of the electrochemical reactor coupled to a photovoltaic system on an enlarged scale. Reprinted from Valero et al. (2014) Copyright (2014), with permission from Elsevier

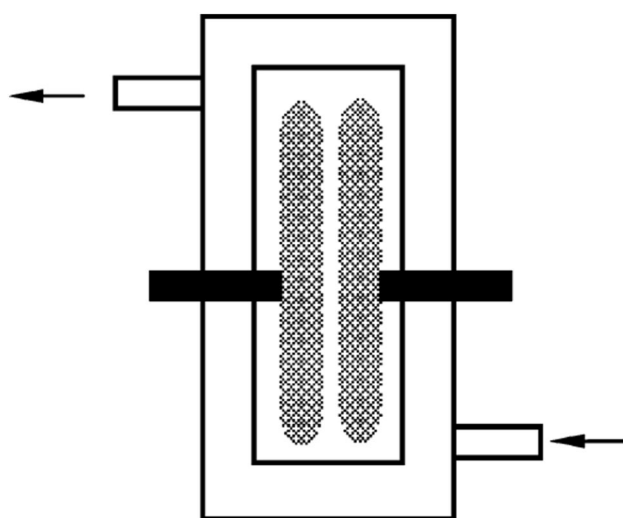


Fig. 6 Proposed flow reactor profile view. Reprinted (adapted) with permission from Vaghela et al. (2005), Copyright (2005) American Chemical Society

elucidation of the possibility of applying this system in real textile effluents containing azo-dyes, which comprise a wide range in the market of transformation.

Another study, developed by Vaghela et al. (2005), proposes the construction and application of a reactor for the electro-oxidation of real effluents containing azo-dyes. In this sense, a rectangular PVC reactor with dimensions (10.5 cm × 6 cm) with inlet and outlet flow was used with an anode (effective area of 50.16 cm²), and a thin stainless-steel plate (11 cm × 8 cm) as cathode. The total volume of contained solution was 100 mL in one system. The effluent containing a mixture between azo-dyes (reactive red 2, reactive red 20, reactive orange 4 and reactive orange 13) was allowed to flow from the bottom of the cell at a certain rate, which was regulated in three flow rates 5, 10 and 15 mL min⁻¹. A current between 0 and 100 mA cm² was applied between the two electrodes while the effluent was constantly fed into the cell. The effluent electrochemically treated was analyzed to estimate the percentage discoloration from the absorption data. The COD decay was determined by a standard method using potassium dichromate. The cell model described by Vaghela and collaborators (2005) can be seen in Fig. 6.

The results obtained by the application of the reactor were satisfactory for the initial purposes—removal of color and attenuation of the chemical oxygen demand of the effluent. For the range of investigated current densities, the decolorization was 85.3 to 99.2% at a flow rate of 5 mL min⁻¹, while at higher flow rates, as 15 mL min⁻¹, for example, the removal reached the lowest values. Furthermore, it was found that for all flow rates investigated, higher values of color removal were found for higher current densities. The

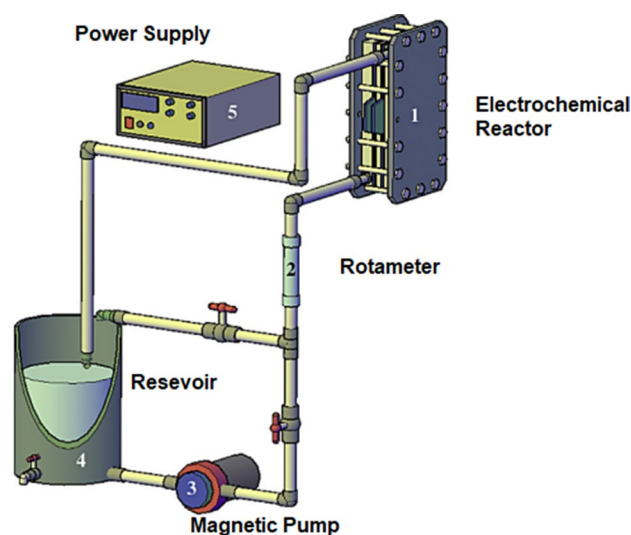


Fig. 7 Scheme for a reactor plant used in the degradation of methyl orange present in textile effluent. Reprinted from Brillas and Martínez-Huitle (2015), Copyright (2015), with permission from Elsevier

evaluation of the reduction in oxygen demand (COD) was carried out as a function of the specific area of the electrode, and it was observed that under conditions of high area and applied current density, the high COD values achieve the summit in 80.8% of decay at $j = 40 \text{ mA cm}^{-2}$ and area of 21.5 cm². Although the authors have obtained satisfactory results, the flow reactor presents the use of Polyvinyl chloride (PVC) in its structure as a disadvantage. Therefore, because the dyes present high adhesion to polymers, an alternative to the PVC reactors would be the use of systems based on less reactive materials, as highlighted by El-Ghenymy et al. (2014) and Antonin et al. (2015).

Brillas and Martínez-Huitle (2015) and Isarain-Chávez et al. (2013), developed a prototype/reactor plant based on the EAOPs of Electro-Fenton for degradation of the methyl orange azo-dye. In recent years, the electrochemical generation of Fenton's reagent in situ, also known as the electro-Fenton (EF), has been studied in order to achieve high standards of removal of several contaminants. These studies are mainly based on the possibility of reducing dissolved oxygen to hydrogen peroxide under conditions outside of selectivity, *i.e.*, outside the acidic medium (Isarain-Chávez et al. 2013; Brillas and Martínez-Huitle 2015). Regarding the developed plant, for each test performed, about 3 L of real effluent solution was introduced into the reservoir and recirculated in the system by means of a centrifugal pump at a flow rate of 12 L min⁻¹, controlled by a rotameter. The electrochemical reactor had two BDD diamond-doped boron electrodes as respective cathode and anode. Both rectangular plate electrodes, with a geometric area of 64 cm² and a distance of 2.5 cm each other, were put in contact with the 0.05 mol L⁻¹ Na₂SO₄ solution. Before the degradation

Table 6 Different electrochemical systems in a pilot plant and on a larger scale applied to the evaluation of the efficiency of the degradation process of azo-dyes present in synthetic effluents

Azo-dye	Pollutant characteristics	Electrochemical processes/scale	Parameters	Removal efficiency (%)	References
Methyl Red, Orange II, Biebrich Scarlett azo dyes	100 mg L ⁻¹ in each dye solution	EF (Pilot-scale)	Anode: Pt (31.4 cm ²) Cathode: Carbon Felt (42 or 378 cm ²) E: -0.5 V Flow Rate: 5,8 L min ⁻¹ ; T: 303 K pH: 1.0 or 3.0	11%	Elias et al. (2011)
Methyl violet 2B dye	69–548 mg Methyl violet 2B L ⁻¹ in 7.0 g Na ₂ SO ₄ L ⁻¹	EO (Pilot-scale)	Anode: BDD ^a or Pt (3 cm ²) Cathode: Pt (3 cm ²) j: 33–150 mA cm ⁻² Flow rate: stirring T: 308 K pH: 3.0 or 7.4	74%	Hamza et al. (2009)
Acid violet 7	200 mg acid Violet 7 L ⁻¹ in 0.05 mol L ⁻¹ Na ₂ SO ₄	EO	Anode: BDD/Nb (63.5 cm ²) Cathode: Ti j: 15–60 mA cm ⁻² Flow Rate: 2,67 L min ⁻¹ T: 298 K pH: 7.2	> 82%	Brito et al. (2018)
Reactive orange 16, reactive red 120, direct red 80 (mixture)	100–400 mg L ⁻¹ in Na ₂ SO ₄	EO	Anode: SS Cathode: SS j: 47.00 mA cm ⁻² Flow rate: 0.0017 – 0.0082 L min ⁻¹ T: 298 K pH: 3.0 – 7.0	> 98%	Alagesan et al. (2021)
Methyl orange	10.00–50.00 mg L ⁻¹ in 0.1 mol L ⁻¹ NaClO ₄	Photo-EO	Anode: TiO ₂ Nanotubular Cathode: Ti Platini-zaded j: 0.14–2.5 mA Flow rate: 0.007 – 0.120 L min ⁻¹ T: 298 K pH: 3.0 – 7.0	> 70%	Mais et al. (2020)
Orange G azo dye	294–3580 mg Orange G L ⁻¹ in 7.0 g Na ₂ SO ₄ L ⁻¹	EO (pilot-scale)	Anode: BDD ^a (3 cm ²) Cathode: SS ^c (3 cm ²) j: 33–150 mA cm ⁻² Flow Rate: 11 mL min ⁻¹ T: 35 °C pH: 2.0–6.0	99.8%	El-Ghenymy et al. (2014)
Indigo dye	315 mg Indigo L ⁻¹ in 2.9 g NaCl L ⁻¹	EO (pilot-scale)	Anode: 2D (plate) BDD ^a (64 cm ²) or 3D (mesh) BDD ^a (444 cm ²) Cathode: Pt j: 5.6 or 15 mA cm ⁻² Flow Rate: 0.10–1.1 L min ⁻¹ T: 25 °C pH: 6.3	Approx. 30 – 60%	Nava et al. (2014)

Table 6 (continued)

Azo-dye	Pollutant characteristics	Electrochemical processes/scale	Parameters	Removal efficiency (%)	References
Evans blue azo dye	235 mg Evans blue L ⁻¹ in 7.0 g Na ₂ SO ₄ L ⁻¹	EF PEF SPEF	Anode: Pt (90.3 cm ²) Cathode: C-PTFE ^b (90.3 cm ²) <i>j</i> : 100 mA cm ⁻² Flow rate: 3.3 L min ⁻¹ T: 35 °C pH: 3.0	75% 88% 90%	Antonin et al. (2015)
Acid yellow 36 azo dye	20 mg Acid yellow 36 L ⁻¹ + 5 mg kaolin L ⁻¹ in 1.1 g KCl L ⁻¹	EO (Pilot scale)	Anode: BDD ^a (9.4 cm ²) Cathode: Carbon felt <i>j</i> : 30 mA cm ⁻² Flow rate: 1.3 L min ⁻¹ T: 25 °C pH: 3.0	Approx. 30%	Juang et al. (2013)

^aBDD Boron-doped diamond electrode

^bC-PTFE: Carbon- polytetrafluoroethylene electrode

^cSS Stainless Steel Electrodes

experiments, the Na₂SO₄ solution was electrolyzed in the plant at 50 mA cm⁻² for 60 min to remove surface impurities BDD (Cruz-González et al. 2010; Ruiz et al. 2011). Figure 7 allows a better verification of the system used by the authors.

The aforementioned treatment allowed to determine the behavior of the applied current against removal by electrolysis time. The experimental data demonstrated that the oxidation rate and process efficiency are proportional to the concentration of the azo-dye, as well as evaluated in empirical kinetic profiles. Maximum efficiencies were obtained during the early stages of the process, with a subsequent loss of efficiency during the experiment, reaching a steady state. According to the authors, this behavior is characteristic of the electrochemical oxidation of wastewater using the EF technique, both in flow cells and in pre-established batches. The greatest decolorization efficiency was obtained by applying 31 mA cm⁻². Therefore, methyl orange is rapidly decolorized during the first 10 min under these conditions, yielding 80% decolorization efficiency. On the other hand, the use of current densities of 7.8 and 15 mA cm⁻² lead to 70% and 60% decolorization efficiency, respectively, slightly reducing overall performance. Take into account the energy consumption, the developed system presented an energy consumption of 7.66 kWh m⁻³, which is considered moderately low.

A positive point in the article explanations is the identification of by-products from the electro-oxidative process. Thus, generated carboxylic acids such as ascorbic, benzoic, citric, maleic and oxalic were detected by ion exclusion HPLC (Isarain-Chávez et al. 2013). However, considering the energy demand for the Electro-Fenton procedure

associated with BDD electrodes in a flow system, it is necessary to dispose of renewable and eco-friendly sources of electricity to operate this device. The setup powered by hybrid technology, such as the association of photovoltaic systems, for example, could be an alternative for overcoming the cost limitations. This idea, already supported by Valero et al. (2014) in apparatus using commercial DSA and a flow system, can be easily migrated to the displayed plant, being even more functional and energetically economical.

Table 6 shows other studies about the degradation of azo-dyes present in real or synthetic effluents, regarding the scaling-up applications for electro-oxidative systems.

Conclusion

The pollution of water resources has been a major issue nowadays, mainly when dealing with pollution caused by dyes from the azo group. These species permeate into trophic levels and cause devastating problems, from the death of marine animals by eutrophication to profound changes in DNA. Due to this problem, it has become increasingly necessary to search for effective methodologies to minimize these effects. Taking this into account, the use of methodologies based on EAOPs has gained a lot of attention today because it is a viable alternative for the removal of azo-dyes present in different matrices. In terms of removal efficiency, EAOPs have been frequently reported in the literature as techniques that allow obtaining high removal rates, very efficient water remediation, and low energy consumption. In the present review, it was possible to verify that the application of

techniques such as Electrochemical oxidation (EO), Electro-Fenton (EF), Heterogeneous Electro-Fenton (HEF), Photoelectro-Fenton (PEF), and Solar Photoelectro-Fenton (SPEF) are powerful technologies for the treatment of contaminated effluents by dyes. These technologies show color removals in the range of 80%–90% and a drastic reduction in COD, BOD, and TOC. Such parameters are taken as real evidence to assess the extent of the degradation procedure. In fact, it is clear that even with the advances in electrochemical purification techniques, it is still necessary for more studies in order to develop more stable catalysts, with longer lifetimes, and high catalytic activity. In this sense, the modulation of electrocatalyst properties combined with scale-up design may reduce costs and improve the efficiency parameters of EAOPs to even higher levels compared to those reported in the literature so far. Further studies must also be devoted for understanding of the degradation and by-product formation processes since the dyes are usually present in a complex mixture of chemical species and interactions or recombination can yield in more toxic compounds. In addition to this, the efforts addressed to the design of hybrid systems based on EAOPs will allow the development of novel technologies for water treatment at an industrial scale. Thus, we conclude in this review that the EAOPs are versatile and effective wastewater treatment with dye contents, but many efforts still have to be taken so that the acceptability of these techniques is increasing within the textile industrial scope, in post-transformation stages, guaranteeing great benefits in financial and environmental shortly.

Acknowledgements This work was supported by the Coordenação de Aperfeiçoamento de Pessoal de Nível Superior—Brasil (CAPES) [Finance Code 001], Conselho Nacional de Desenvolvimento Científico e Tecnológico (CNPq), and Fundação de Amparo à Pesquisa e Inovação do Espírito Santo (FAPES).

Data availability The datasets generated during and/or analyzed during the current study are available from the corresponding author upon reasonable request. All data generated or analyzed during this study are included in this published article (and its supplementary information files).

Declarations

Conflict of interest The authors declare that they have no known competing financial interests or personal relationships that could have appeared to influence the work reported in this paper.

Ethics approval Not applicable.

Consent to participate Not applicable.

Consent for publication Not applicable.

References

- Adachi A, El OF, Kara M et al (2022) Decolorization and degradation of methyl orange Azo Dye in aqueous solution by the electro-fenton process: application of optimization. *Catalysts* 12:665. <https://doi.org/10.3390/catal12060665>
- Adams JS, Kromer ML, Rodríguez-López J, Flaherty DW (2021) Unifying concepts in electro- and thermocatalysis toward hydrogen peroxide production. *J Am Chem Soc* 143:7940–7957. <https://doi.org/10.1021/jacs.0c13399>
- Adedayo O, Javadpour S, Taylor C et al (2004) Decolourization and detoxification of methyl red by aerobic bacteria from a wastewater treatment plant. *World J Microbiol Biotechnol* 20:545–550. <https://doi.org/10.1023/B:WIBI.0000043150.37318.5f>
- Afanga H, Zazou H, Titchou FE et al (2021) Electrochemical oxidation of Naphthol Blue Black with different supporting electrolytes using a BDD /carbon felt cell. *J Environ Chem Eng* 9:104498. <https://doi.org/10.1016/j.jece.2020.104498>
- Aguilar ZG, Coreño O, Salazar M et al (2018) TiIr–Sn–Sb oxide anode: Service life and role of the acid sites content during water oxidation to hydroxyl radicals. *J Electroanal Chem* 820:82–88. <https://doi.org/10.1016/j.jelechem.2018.04.053>
- Ahmed Basha C, Soloman PA, Velan M et al (2010) Electrochemical degradation of specialty chemical industry effluent. *J Hazard Mater* 176:154–164. <https://doi.org/10.1016/j.jhazmat.2009.10.131>
- Alagesan J, Jaisankar M, Muthuramalingam S et al (2021) Influence of number of azo bonds and mass transport limitations towards the elimination capacity of continuous electrochemical process for the removal of textile industrial dyes. *Chemosphere* 262:128381. <https://doi.org/10.1016/j.chemosphere.2020.128381>
- Alcocer S, Picos A, Uribe AR et al (2018) Comparative study for degradation of industrial dyes by electrochemical advanced oxidation processes with BDD anode in a laboratory stirred tank reactor. *Chemosphere* 205:682–689. <https://doi.org/10.1016/j.chemosphere.2018.04.155>
- Almeida LC, Garcia-Segura S, Arias C et al (2012) Electrochemical mineralization of the azo dye Acid Red 29 (Chromotrope 2R) by photoelectro-Fenton process. *Chemosphere* 89:751–758. <https://doi.org/10.1016/j.chemosphere.2012.07.007>
- Antonin VS, Garcia-Segura S, Santos MC, Brillias E (2015) Degradation of Evans Blue diazo dye by electrochemical processes based on Fenton's reaction chemistry. *J Electroanal Chem* 747:1–11. <https://doi.org/10.1016/j.jelechem.2015.03.032>
- Aveiro LR, Da Silva AGM, Candido EG et al (2018) Application and stability of cathodes with manganese dioxide nanoflowers supported on Vulcan by Fenton systems for the degradation of RB5 azo dye. *Chemosphere* 208:131–138. <https://doi.org/10.1016/j.chemosphere.2018.05.107>
- Avlonitis SA, Kouroumbas K, Vlachakis N (2003) Energy consumption and membrane replacement cost for seawater RO desalination plants. *Desalination* 157:151–158. [https://doi.org/10.1016/S0011-9164\(03\)00395-3](https://doi.org/10.1016/S0011-9164(03)00395-3)
- Azarian G, Miri M, Nematollahi D (2018) Combined electrocoagulation/electrooxidation process for the COD removal and recovery of tannery industry wastewater. *Environ Prog Sustain Energy* 37:637–644. <https://doi.org/10.1002/ep.12711>
- Baban A, Yediler A, Lienert D et al (2003) Ozonation of high strength segregated effluents from a woollen textile dyeing and finishing plant. *Dye Pigment* 58:93–98. [https://doi.org/10.1016/S0143-7208\(03\)00047-0](https://doi.org/10.1016/S0143-7208(03)00047-0)
- Babu DS, Srivastava V, Nidheesh PV, Kumar MS (2019) Detoxification of water and wastewater by advanced oxidation processes.

- Sci Total Environ 696:133961. <https://doi.org/10.1016/j.scitotenv.2019.133961>
- Babunpusami A, Muthukumar K (2013) Treatment of phenol-containing wastewater by photoelectro-Fenton method using supported nanoscale zero-valent iron. *Environ Sci Pollut Res* 20:1596–1605. <https://doi.org/10.1007/s11356-012-0990-1>
- Baddouh A, Bessegato GG, Rguiti MM et al (2018) Electrochemical decolorization of Rhodamine B dye: Influence of anode material, chloride concentration and current density. *J Environ Chem Eng* 6:2041–2047. <https://doi.org/10.1016/j.jece.2018.03.007>
- Bafana A, Devi SS, Chakrabarti T (2011) Azo dyes: past, present and the future. *Environ Rev* 19:350–371. <https://doi.org/10.1139/a11-018>
- Baran MJ, Braten MN, Sahu S et al (2019) Design rules for membranes from polymers of intrinsic microporosity for crossover-free aqueous electrochemical devices. *Joule* 3:2968–2985. <https://doi.org/10.1016/j.joule.2019.08.025>
- Barhoum A, Favre T, Sayegh S et al (2021) 3D Self-supported nitrogen-doped carbon nanofiber electrodes incorporated Co/CoOx nanoparticles: application to dyes degradation by electro-fenton-based process. *Nanomaterials* 11:2686. <https://doi.org/10.3390/nano11102686>
- Beharry AA, Woolley GA (2011) Azobenzene photoswitches for biomolecules. *Chem Soc Rev* 40:4422–4437
- Bello MM, Abdul Raman AA, Asghar A (2019) A review on approaches for addressing the limitations of Fenton oxidation for recalcitrant wastewater treatment. *Process Saf Environ Prot* 126:119–140. <https://doi.org/10.1016/j.psep.2019.03.028>
- Benhadji A, Ahmed MT (2020) Yellow 2G dye degradation by electro-Fenton process using steel electrode as catalysis and its phytotoxicity effect. *Water Sci Technol*. <https://doi.org/10.2166/wst.2020.361>
- Blanco J, Torrades F, Morón M et al (2014) Photo-Fenton and sequencing batch reactor coupled to photo-Fenton processes for textile wastewater reclamation: Feasibility of reuse in dyeing processes. *Chem Eng J* 240:469–475. <https://doi.org/10.1016/j.cej.2013.10.101>
- Bonfatti F, De Battisti A, Ferro S et al (2000) Anodic mineralization of organic substrates in chloride-containing aqueous media. *Electrochim Acta* 46:305–314. [https://doi.org/10.1016/S0013-4686\(00\)00586-7](https://doi.org/10.1016/S0013-4686(00)00586-7)
- Boodts JFC, Trasatti S (1990) Effect of composition on the electrocatalytic activity of the ternary oxide Ru_{0.3}Ti_(0.7-x)Sn_xO₂: I. Oxygen evolution from solutions. *J Electrochem Soc* 137:3784–3789. <https://doi.org/10.1149/1.2086301>
- Borràs N, Arias C, Oliver R, Brillas E (2013) Anodic oxidation, electro-Fenton and photoelectro-Fenton degradation of cyanazine using a boron-doped diamond anode and an oxygen-diffusion cathode. *J Electroanal Chem* 689:158–167. <https://doi.org/10.1016/j.jelechem.2012.11.012>
- Bravo-Yumi N, Espinoza-Montero P, Picos-Benítez A et al (2020) Synthesis and characterization of Sb₂O₅-doped Ti/SnO₂-IrO₂ anodes toward efficient degradation tannery dyes by in situ generated oxidizing species. *Electrochim Acta* 358:136904. <https://doi.org/10.1016/j.electacta.2020.136904>
- Brillas E (2014) A review on the degradation of organic pollutants in waters by UV photoelectro-fenton and solar photoelectro-fenton. *J Brazilian Chem Soc* 25:393–417
- Brillas E (2020) A review on the photoelectro-Fenton process as efficient electrochemical advanced oxidation for wastewater remediation. Treatment with UV light, sunlight, and coupling with conventional and other photo-assisted advanced technologies. *Chemosphere* 250:126198. <https://doi.org/10.1016/j.chemosphere.2020.126198>
- Brillas E (2021) Recent development of electrochemical advanced oxidation of herbicides. A review on its application to wastewater treatment and soil remediation. *J Clean Prod* 290:125841. <https://doi.org/10.1016/j.jclepro.2021.125841>
- Brillas E, Martínez-Huitile CA (2015) Decontamination of wastewaters containing synthetic organic dyes by electrochemical methods. An updated review. *Appl Catal B Environ* 166–167:603–643. <https://doi.org/10.1016/j.apcatb.2014.11.016>
- Brillas E, Sirés I, Oturan MA (2009) Electro-Fenton process and related electrochemical technologies based on fenton's reaction chemistry. *Chem Rev* 109:6570–6631. <https://doi.org/10.1021/cr900136g>
- Brito CN, Ferreira MB, de Moura Santos ECM et al (2018) Electrochemical degradation of Azo-dye Acid Violet 7 using BDD anode: effect of flow reactor configuration on cell hydrodynamics and dye removal efficiency. *J Appl Electrochem* 48:1321–1330. <https://doi.org/10.1007/s10800-018-1257-4>
- Bustos-Terrones YA, Hermosillo-Nevárez JJ, Ramírez-Pereda B et al (2021) Removal of BB9 textile dye by biological, physical, chemical, and electrochemical treatments. *J Taiwan Inst Chem Eng* 121:29–37. <https://doi.org/10.1016/j.jtice.2021.03.041>
- Cañizares P, García-Gómez J, Fernández de Marcos I et al (2006) Measurement of mass-transfer coefficients by an electrochemical technique. *J Chem Educ* 83:1204. <https://doi.org/10.1021/ed083p1204>
- Catino SC, Farris E (1985) Concise encyclopedia of chemical technology.
- Cavalcanti EB, Garcia-Segura S, Centellas F, Brillas E (2013) Electrochemical incineration of omeprazole in neutral aqueous medium using a platinum or boron-doped diamond anode: degradation kinetics and oxidation products. *Water Res* 47:1803–1815. <https://doi.org/10.1016/j.watres.2013.01.002>
- Çelebi MS, Oturan N, Zazou H et al (2015) Electrochemical oxidation of carbaryl on platinum and boron-doped diamond anodes using electro-Fenton technology. *Sep Purif Technol* 156:996–1002. <https://doi.org/10.1016/j.seppur.2015.07.025>
- Chekir N, Benhabiles O, Tassalit D et al (2016) Photocatalytic degradation of methylene blue in aqueous suspensions using TiO₂ and ZnO. *Desalin Water Treat* 57:6141–6147. <https://doi.org/10.1080/19443994.2015.1060533>
- Clarke EA, Anliker R (1980) Organic Dyes and Pigments. pp 181–215.
- Coha M, Farinelli G, Tiraferri A et al (2021) Advanced oxidation processes in the removal of organic substances from produced water: Potential, configurations, and research needs. *Chem Eng J* 414:128668. <https://doi.org/10.1016/j.cej.2021.128668>
- Coledam DAC, Sanchez-Montes I, Silva BF, Aquino JM (2018) On the performance of HOCl/Fe²⁺, HOCl/Fe²⁺/UVA, and HOCl/UVC processes using in situ electrogenerated active chlorine to mineralize the herbicide picloram. *Appl Catal B Environ* 227:170–177
- Cominellis C, Pulgarin C (1993) Electrochemical oxidation of phenol for wastewater treatment using SnO₂ anodes. *J Appl Electrochem*. <https://doi.org/10.1007/BF00246946>
- Cominellis C, Vercesi GP (1991) Characterization of DSA-type oxygen evolving electrodes: choice of a coating. *J Appl Electrochem* 21:335–345. <https://doi.org/10.1007/BF01020219>
- Corona-Bautista M, Picos-Benítez A, Villaseñor-Basulto D et al (2021) Discoloration of azo dye brown HT using different advanced oxidation processes. *Chemosphere* 267:129234. <https://doi.org/10.1016/j.chemosphere.2020.129234>
- Cotillas S, Llanos J, Cañizares P et al (2019) Removal of Procion Red MX-5B dye from wastewater by conductive-diamond electrochemical oxidation. *Electrochim Acta* 263:1–7. <https://doi.org/10.1016/j.electacta.2018.01.052>
- Coura JC, Profeti D, Profeti LPR (2020) Eco-friendly chitosan/quartzite composite as adsorbent for dye removal. *Mater Chem Phys*

- 256:123711. <https://doi.org/10.1016/j.matchemphys.2020.123711>
- Cruz DRS, de Jesus GK, Santos CA et al (2021) Magnetic nanostructured material as heterogeneous catalyst for degradation of AB210 dye in tannery wastewater by electro-Fenton process. *Chemosphere* 280:130675. <https://doi.org/10.1016/j.chemosphere.2021.130675>
- Cruz-González K, Torres-López O, García-León A et al (2010) Determination of optimum operating parameters for acid yellow 36 decolorization by electro-Fenton process using BDD cathode. *Chem Eng J* 160:199–206. <https://doi.org/10.1016/j.ccej.2010.03.043>
- da Silva RG, de Andrade AR (2015) Degradation of the dye reactive blue 4 by coupled photoassisted electrochemistry at DSA®-type electrode. *J Braz Chem Soc*. <https://doi.org/10.5935/0103-5053.20150338>
- da Costa Soares IC, da Silva DR, do Nascimento JHO, et al (2017) Functional group influences on the reactive azo dye decolorization performance by electrochemical oxidation and electro-Fenton technologies. *Environ Sci Pollut Res* 24:24167–24176. <https://doi.org/10.1007/s11356-017-0041-z>
- de Araújo KS, Antonelli R, Gaydeczka B et al (2016) Processos oxidativos avançados: uma revisão de fundamentos e aplicações no tratamento de águas residuais urbanas e efluentes industriais. *Rev Ambient Água* 11:387–401
- de Araújo KC, F, Barreto JP de P, Cardozo JC, et al (2018) Sulfate pollution: evidence for electrochemical production of persulfate by oxidizing sulfate released by the surfactant sodium dodecyl sulfate. *Environ Chem Lett* 16:647–652. <https://doi.org/10.1007/s10311-017-0703-6>
- de Moraes CC, O, da Silva AJC, Ferreira MB, et al (2013) Electrochemical degradation of methyl red using Ti/Ru_{0.3}Ti_{0.7}O₂: Fragmentation of Azo Group. *Electrocatalysis* 4:312–319. <https://doi.org/10.1007/s12678-013-0166-x>
- del Río AI, Molina J, Bonastre J, Cases F (2009) Influence of electrochemical reduction and oxidation processes on the decolourisation and degradation of C.I. Reactive Orange 4 solutions. *Chemosphere* 75:1329–1337. <https://doi.org/10.1016/j.chemosphere.2009.02.063>
- Dhakshinamoorthy A, Navalon S, Alvaro M, Garcia H (2012) Metal nanoparticles as heterogeneous Fenton catalysts. *Chemosphere* 5:46–64. <https://doi.org/10.1002/cssc.201100517>
- dos Santos AJ, da Costa CG, Cruz DRS et al (2019) Iron mining wastes collected from Mariana disaster: Reuse and application as catalyst in a heterogeneous electro-Fenton process. *J Electroanal Chem* 848:113330. <https://doi.org/10.1016/j.jelechem.2019.113330>
- Duan F, Li Y, Cao H et al (2015) Activated carbon electrodes: Electrochemical oxidation coupled with desalination for wastewater treatment. *Chemosphere* 125:205–211. <https://doi.org/10.1016/j.chemosphere.2014.12.065>
- Dung NT, Duong LT, Hoa NT et al (2022) A comprehensive study on the heterogeneous electro-Fenton degradation of tartrazine in water using CoFe₂O₄/carbon felt cathode. *Chemosphere* 287:132141. <https://doi.org/10.1016/j.chemosphere.2021.132141>
- Eden RE (1996) Wastewater reuse-limitations and possibilities. *Desalination* 106:335–338
- Elaissaoui I, Akrouit H, Grassini S et al (2019) Effect of coating method on the structure and properties of a novel PbO₂ anode for electrochemical oxidation of Amaranth dye. *Chemosphere* 217:26–34. <https://doi.org/10.1016/j.chemosphere.2018.10.161>
- El-Ghenymy A, Centellas F, Garrido JA et al (2014) Decolorization and mineralization of Orange G azo dye solutions by anodic oxidation with a boron-doped diamond anode in divided and undivided tank reactors. *Electrochim Acta* 130:568–576. <https://doi.org/10.1016/j.electacta.2014.03.066>
- Elias B, Guihard L, Nicolas S et al (2011) Effect of electro-Fenton application on azo dyes biodegradability. *Environ Prog Sustain Energy* 30:160–167. <https://doi.org/10.1002/ep.10457>
- Eren Z, Acar FN (2007) Equilibrium and kinetic mechanism for Reactive Black 5 sorption onto high lime soma fly ash. *J Hazard Mater* 143:226–232. <https://doi.org/10.1016/j.jhazmat.2006.09.017>
- Ferro S, Rosetolato D, Martínez-Huitle CA, De Battisti A (2014) On the oxygen evolution reaction at IrO₂-SnO₂ mixed-oxide electrodes. *Electrochim Acta* 146:257–261. <https://doi.org/10.1016/j.electacta.2014.08.110>
- Galizzioli D, Trasatti S (1973) Work function, electronegativity, and electrochemical behaviour of metals. *J Electroanal Chem Interfacial Electrochem* 44:367–388. [https://doi.org/10.1016/S0022-0728\(73\)80469-3](https://doi.org/10.1016/S0022-0728(73)80469-3)
- Galizzioli D, Tantardini F, Trasatti S (1975) Ruthenium dioxide: a new electrode material. II. non-stoichiometry and energetics of electrode reactions in acid solutions. *J Appl Electrochem* 5:203–214. <https://doi.org/10.1007/BF01637270>
- Ganiyu SO, Zhou M, Martínez-Huitle CA (2018) Heterogeneous electro-Fenton and photoelectro-Fenton processes: a critical review of fundamental principles and application for water/wastewater treatment. *Appl Catal B Environ* 235:103–129. <https://doi.org/10.1016/j.apcatb.2018.04.044>
- García-Segura S, Brillas E (2016) Combustion of textile monoazo, diazo and triazo dyes by solar photoelectro-Fenton: decolorization, kinetics and degradation routes. *Appl Catal B Environ* 181:681–691. <https://doi.org/10.1016/j.apcatb.2015.08.042>
- García-Segura S, Ocon JD, Chong MN (2018) Electrochemical oxidation remediation of real wastewater effluents — a review. *Process Saf Environ Prot* 113:48–67. <https://doi.org/10.1016/j.psep.2017.09.014>
- Gargouri B, Gargouri OD, Gargouri B et al (2014) Application of electrochemical technology for removing petroleum hydrocarbons from produced water using lead dioxide and boron-doped diamond electrodes. *Chemosphere* 117:309–315. <https://doi.org/10.1016/j.chemosphere.2014.07.067>
- GilPavas E, Correa-Sánchez S (2019) Optimization of the heterogeneous electro-Fenton process assisted by scrap zero-valent iron for treating textile wastewater: assessment of toxicity and biodegradability. *J Water Process Eng* 32:100924. <https://doi.org/10.1016/j.jwpe.2019.100924>
- Gonzalez, I. L., Moreira, J. A., de Andrade, A. R., & Ribeiro, J. (2016). Estudo da Reação de Desprendimento de Oxigênio em Eletrodos do Tipo Ta/RuO₂-Ta₂O₅-TiO₂. *Rev Virtual Quim*, 8(5):1347–1365. <https://doi.org/10.21577/1984-6835.20160096>.
- Girrane A, Corma A, García H (2008) Gold-catalyzed synthesis of aromatic azo compounds from anilines and nitroaromatics. *Science* 322:1661–1664. <https://doi.org/10.1126/science.1166401>
- Guaratini CCI, Zanoni MVB (2010) Corantes têxteis. *Quim Nova* 23:71–78. <https://doi.org/10.1590/S0100-4042200000100013>
- Guimarães T, Paquini LD, Lyrio Ferraz BR et al (2020) Efficient removal of Cu(II) and Cr(III) contaminants from aqueous solutions using marble waste powder. *J Environ Chem Eng* 8:103972. <https://doi.org/10.1016/j.jece.2020.103972>
- Gung BW, Taylor RT (2004) Parallel combinatorial synthesis of azo dyes: a combinatorial experiment suitable for undergraduate laboratories. *J Chem Educ* 81:1630. <https://doi.org/10.1021/ed081p1630>
- Hamza M, Abdelhedi R, Brillas E, Sirés I (2009) Comparative electrochemical degradation of the triphenylmethane dye Methyl Violet with boron-doped diamond and Pt anodes. *J Electroanal Chem* 627:41–50. <https://doi.org/10.1016/j.jelechem.2008.12.017>

- He W, Ma Q, Wang J et al (2014a) Preparation of novel kaolin-based particle electrodes for treating methyl orange wastewater. *Appl Clay Sci* 99:178–186. <https://doi.org/10.1016/j.clay.2014a.06.030>
- He Z, Gao C, Qian M et al (2014b) Electro-Fenton process catalyzed by Fe₃O₄ magnetic nanoparticles for degradation of C.I. Reactive Blue 19 in aqueous solution: operating conditions, influence, and mechanism. *Ind Eng Chem Res* 53:3435–3447. <https://doi.org/10.1021/ie403947b>
- Horváth O, Stevenson KL (1993) Charge transfer photochemistry of coordination compounds. Wiley-VCH
- Huang J, Ling J, Kuang C et al (2018) Microbial biodegradation of aniline at low concentrations by *Pigmentiphaga daeguensis* isolated from textile dyeing sludge. *Int Biodeterior Biodegradation* 129:117–122. <https://doi.org/10.1016/j.ibiod.2018.01.013>
- Ibrahim SA, El-Gahami MA, Khafagi ZA, El-Gyar SA (1991) Structure and antimicrobial activity of some new azopyrazolone chelates of Ni (II) and Cu (II) acetates, sulfates, and nitrates. *J Inorg Biochem* 43:1–7. [https://doi.org/10.1016/0162-0134\(91\)84063-f](https://doi.org/10.1016/0162-0134(91)84063-f)
- Iranifam M, Zarei M, Khataee AR (2011) Decolorization of C.I. Basic Yellow 28 solution using supported ZnO nanoparticles coupled with photoelectro-Fenton process. *J Electroanal Chem* 659:107–112. <https://doi.org/10.1016/j.jelechem.2011.05.010>
- Isarain-Chávez E, De La Rosa C, Martínez-Huitle CA, Peralta-Hernández JM (2013) On-site hydrogen peroxide production at pilot flow plant: application to electro-Fenton process. *Int J Electrochem Sci* 8:3084–3094
- Isarain-Chávez E, Baró MD, Rossinyol E et al (2017) Comparative electrochemical oxidation of methyl orange azo dye using Ti/Ir-Pb, Ti/Ir-Sn, Ti/Ru-Pb, Ti/Pt-Pd and Ti/RuO₂ anodes. *Electrochim Acta* 244:199–208. <https://doi.org/10.1016/j.electacta.2017.05.101>
- Javaid R, Qazi UY (2019) Catalytic oxidation process for the degradation of synthetic dyes: an overview. *Int J Environ Res Public Health* 16:2066. <https://doi.org/10.3390/ijerph16112066>
- Jiang H, Sun Y, Feng J, Wang J (2016) Heterogeneous electro-Fenton oxidation of azo dye methyl orange catalyzed by magnetic Fe₃O₄ nanoparticles. *Water Sci Technol* 74:1116–1126. <https://doi.org/10.2166/wst.2016.300>
- Juang Y, Nurhayati E, Huang C et al (2013) A hybrid electrochemical advanced oxidation/microfiltration system using BDD/Ti anode for acid yellow 36 dye wastewater treatment. *Sep Purif Technol* 120:289–295. <https://doi.org/10.1016/j.seppur.2013.09.042>
- Kenova TA, Kornienko GV, Golubtsova OA et al (2018) Electrochemical degradation of Mordant Blue 13 azo dye using boron-doped diamond and dimensionally stable anodes: influence of experimental parameters and water matrix. *Environ Sci Pollut Res* 25:30425–30440. <https://doi.org/10.1007/s11356-018-2977-z>
- Keshavayya J, Pandurangappa M, Ravi BN (2018) Synthesis, characterization and electrochemical investigations of azo dyes derived from 2-amino-6-ethoxybenzothiazole. *Chem Data Collect* 17:13–29
- Khataee AR, Zarei M (2011) Photocatalysis of a dye solution using immobilized ZnO nanoparticles combined with photoelectrochemical process. *Desalination* 273:453–460. <https://doi.org/10.1016/j.desal.2011.01.066>
- Khehra MS, Saini HS, Sharma DK et al (2005) Decolorization of various azo dyes by bacterial consortium. *Dye Pigment* 67:55–61. <https://doi.org/10.1016/j.dyepig.2004.10.008>
- Kong J, Huang W, Yang S et al (2020) Photoelectro-Fenton system including electromagnetic induction electrodeless lamp and black carbon poly tetra fluoro ethylene air-diffusion cathode: degradation kinetics, intermediates and pathway for azo dye. *Chemosphere* 253:126708. <https://doi.org/10.1016/j.chemosphere.2020.126708>
- Kumar D, Gupta SK (2022) Electrochemical oxidation of direct blue 86 dye using MMO coated Ti anode: modelling, kinetics and degradation pathway. *Chem Eng Process - Process Intensif* 181:109127. <https://doi.org/10.1016/j.ccep.2022.109127>
- Kyzioł-Komosińska J, Augustynowicz J, Lasek W et al (2018) Callitriche cophocarpa biomass as a potential low-cost biosorbent for trivalent chromium. *J Environ Manage* 214:295–304. <https://doi.org/10.1016/j.jenvman.2018.03.010>
- Labiadh L, Oturan MA, Panizza M et al (2015) Complete removal of AHPS synthetic dye from water using new electro-fenton oxidation catalyzed by natural pyrite as heterogeneous catalyst. *J Hazard Mater* 297:34–41. <https://doi.org/10.1016/j.jhazmat.2015.04.062>
- Lee Y, Gerrity D, Lee M et al (2016) Organic contaminant abatement in reclaimed water by UV/H₂O₂ and a combined process consisting of O₃/H₂O₂ Followed by UV/H₂O₂: prediction of abatement efficiency, energy consumption, and byproduct formation. *Environ Sci Technol* 50:3809–3819. <https://doi.org/10.1021/acs.est.5b04904>
- Li F, Xia Q, Cheng Q et al (2017) Conductive cotton filters for affordable and efficient water purification. *Catalysts* 7:291. <https://doi.org/10.3390/catal7100291>
- Li H, Xing X, Wang K et al (2018) Improved BDD anode system in electrochemical degradation of p-nitrophenol by corroding electrode of iron. *Electrochim Acta* 291:335–342. <https://doi.org/10.1016/j.electacta.2018.09.128>
- Liu C-F, Huang CP, Juang Y et al (2019) Graphite supported stainless-steel electrode for the degradation of Azo Dye Orange G by Fenton reactions: effect of photo-irradiation. *J Environ Eng*. [https://doi.org/10.1061/\(ASCE\)EE.1943-7870.0001476](https://doi.org/10.1061/(ASCE)EE.1943-7870.0001476)
- Liu Y, Zhao Y, Wang J (2021) Fenton/Fenton-like processes with in-situ production of hydrogen peroxide/hydroxyl radical for degradation of emerging contaminants: advances and prospects. *J Hazard Mater* 404:124191. <https://doi.org/10.1016/j.jhazmat.2020.124191>
- Ma H, Zhuo Q, Wang B (2009) Electro-catalytic degradation of methylene blue wastewater assisted by Fe₂O₃-modified kaolin. *Chem Eng J* 155:248–253. <https://doi.org/10.1016/j.cej.2009.07.049>
- Mais L, Vacca A, Mascia M et al (2020) Experimental study on the optimisation of azo-dyes removal by photo-electrochemical oxidation with TiO₂ nanotubes. *Chemosphere* 248:125938. <https://doi.org/10.1016/j.chemosphere.2020.125938>
- Malakootian M, Moridi A (2019) Efficiency of electro-Fenton process in removing Acid Red 18 dye from aqueous solutions. *Process Saf Environ Prot* 111:138–147. <https://doi.org/10.1016/j.psep.2017.06.008>
- Márquez AA, Sirés I, Brillas E, Nava JL (2020) Mineralization of Methyl Orange azo dye by processes based on H₂O₂ electro-generation at a 3D-like air-diffusion cathode. *Chemosphere* 259:127466. <https://doi.org/10.1016/j.chemosphere.2020.127466>
- Martínez-Huitle CA, Brillas E (2009) Decontamination of wastewaters containing synthetic organic dyes by electrochemical methods: a general review. *Appl Catal B Environ* 87:105–145. <https://doi.org/10.1016/j.apcatb.2008.09.017>
- Martinez-Huitle CA, Ferro S (2006) Electrochemical oxidation of organic pollutants for the wastewater treatment: direct and indirect processes. *Chem Soc Rev* 35:1324–1340. <https://doi.org/10.1039/B517632H>
- Michael-Kordatou I, Michael C, Duan X et al (2015) Dissolved effluent organic matter: characteristics and potential implications in wastewater treatment and reuse applications. *Water Res* 77:213–248. <https://doi.org/10.1016/j.watres.2015.03.011>
- Moreira FC, Garcia-Segura S, Vilar VJP et al (2013) Decolorization and mineralization of sunset yellow fcf azo dye by anodic oxidation, electro-fenton, uva photoelectro-fenton and solar

- photoelectro-fenton processes. *Appl Catal B Environ* 142–143:877–890. <https://doi.org/10.1016/j.apcatb.2013.03.023>
- Moreira FC, Boaventura RAR, Brillas E, Vilar VJP (2017) Electrochemical advanced oxidation processes: A review on their application to synthetic and real wastewaters. *Appl Catal B Environ* 202:217–261. <https://doi.org/10.1016/j.apcatb.2016.08.037>
- Mousset E, Trellu C, Olvera-Vargas H et al (2021) Electrochemical technologies coupled with biological treatments. *Curr Opin Electrochem* 26:100668. <https://doi.org/10.1016/j.coelec.2020.100668>
- Murrieta MF, Sirés I, Brillas E, Nava JL (2020) Mineralization of acid red 1 azo dye by solar photoelectro-Fenton-like process using electrogenerated HClO and photoregenerated Fe(II). *Chemosphere* 246:125697. <https://doi.org/10.1016/j.chemosphere.2019.125697>
- Muzyka K, Sun J, Fereja TH et al (2019) Boron-doped diamond: current progress and challenges in view of electroanalytical applications. *Anal Methods* 11:397–414. <https://doi.org/10.1039/C8AY02197J>
- Nancharaiyah YV, Venkata Mohan S, Lens PNL (2015) Metals removal and recovery in bioelectrochemical systems: a review. *Bioresour Technol* 195:102–114. <https://doi.org/10.1016/j.biortech.2015.06.058>
- Nava JL, Sirés I, Brillas E (2014) Electrochemical incineration of indigo. a comparative study between 2D (plate) and 3D (mesh) BDD anodes fitted into a filter-press reactor. *Environ Sci Pollut Res* 21:8485–8492. <https://doi.org/10.1007/s11356-014-2781-3>
- Navalon S, Alvaro M, Garcia H (2010) Heterogeneous Fenton catalysts based on clays, silicas and zeolites. *Appl Catal B Environ* 99:1–26. <https://doi.org/10.1016/j.apcatb.2010.07.006>
- Navalon S, Dhakshinamoorthy A, Alvaro M, Garcia H (2011) Heterogeneous Fenton catalysts based on activated carbon and related materials. *Chemosuschem* 4:1712–1730. <https://doi.org/10.1002/cssc.201100216>
- Neyens E, Baeyens J, Weemaes M, De heyder B, (2003) Pilot-scale peroxidation (H₂O₂) of sewage sludge. *J Hazard Mater* 98:91–106. [https://doi.org/10.1016/S0304-3894\(02\)00287-X](https://doi.org/10.1016/S0304-3894(02)00287-X)
- Nidheesh PV (2018) Removal of organic pollutants by peroxicoagulation. *Environ Chem Lett* 16:1283–1292. <https://doi.org/10.1007/s10311-018-0752-5>
- Nidheesh PV, Gandhimathi R (2012) Trends in electro-Fenton process for water and wastewater treatment: an overview. *Desalination* 299:1–15. <https://doi.org/10.1016/j.desal.2012.05.011>
- Nidheesh PV, Gandhimathi R, Ramesh ST (2013) Degradation of dyes from aqueous solution by Fenton processes: a review. *Environ Sci Pollut Res* 20:2099–2132. <https://doi.org/10.1007/s11356-012-1385-z>
- Nidheesh PV, Syam Babu D, Dasgupta B et al (2020) Treatment of Arsenite-Contaminated Water by Electrochemical Advanced Oxidation Processes. *ChemElectroChem* 7:2418–2423. <https://doi.org/10.1002/celec.202000549>
- Oh B-T, Seo Y-S, Sudhakar D et al (2014) Oxidative degradation of endotoxin by advanced oxidation process (O₃/H₂O₂ & UV/H₂O₂). *J Hazard Mater* 279:105–110. <https://doi.org/10.1016/j.jhazmat.2014.06.065>
- Oller I, Malato S, Sánchez-Pérez JA (2011) Combination of Advanced Oxidation Processes and biological treatments for wastewater decontamination—a review. *Sci Total Environ* 409:4141–4166. <https://doi.org/10.1016/j.scitotenv.2010.08.061>
- Oturán MA, Aaron J-J (2014) Advanced oxidation processes in water/wastewater treatment: principles and applications. a review. *Crit Rev Environ Sci Technol* 44:2577–2641. <https://doi.org/10.1080/10643389.2013.829765>
- Ozturk D, Yilmaz AE (2020) Investigation of electrochemical degradation of Basic Red 13 dye in aqueous solutions based on COD removal: numerical optimization approach. *Int J Environ Sci Technol* 17:3099–3110. <https://doi.org/10.1007/s13762-020-02692-2>
- Pacheco-Álvarez MOA, Picos A, Pérez-Segura T, Peralta-Hernández JM (2019) Proposal for highly efficient electrochemical discoloration and degradation of azo dyes with parallel arrangement electrodes. *J Electroanal Chem* 838:195–203. <https://doi.org/10.1016/j.jelechem.2019.03.004>
- Padmavathy S, Sandhya S, Swaminathan K et al (2003) Comparison of decolorization of reactive azo dyes by microorganisms isolated from various sources. *J Env Sci* 15:628–633
- Pandey A, Singh P, Iyengar L (2007) Bacterial decolorization and degradation of azo dyes. *Int Biodeterior Biodegradation* 59:73–84. <https://doi.org/10.1016/j.ibiod.2006.08.006>
- Paz E, Pinheiro V, Aveiro L et al (2019) Hydrogen peroxide electro-generation by gas diffusion electrode modified with tungsten oxide nanoparticles for degradation of orange II and sunset yellow FCF Azo Dyes. *J Braz Chem Soc.* <https://doi.org/10.21577/0103-5053.20190111>
- Pelinson N de S (2017) Estudo de tratabilidade de lixiviado de aterro sanitário submetido à eletro-oxidação como pré-tratamento a um sistema de lodos ativados operado em batelada. Universidade de São Paulo.
- Peña SV (2017) Water disinfection by electrochemical methods. *Cienc Ergo-Sum* 24:145–151
- Peng Q, Zhao H, Qian L et al (2015) Design of a neutral photo-electro-Fenton system with 3D-ordered macroporous Fe₂O₃/carbon aerogel cathode: high activity and low energy consumption. *Appl Catal B Environ* 174:157–166. <https://doi.org/10.1016/j.apcatb.2015.02.031>
- Pereira GF, El-Ghenymy A, Thiam A et al (2016) Effective removal of Orange-G azo dye from water by electro-Fenton and photo-electro-Fenton processes using a boron-doped diamond anode. *Sep Purif Technol* 160:145–151. <https://doi.org/10.1016/j.seppur.2016.01.029>
- Pham XN, Pham DT, Ngo HS et al (2021) Characterization and application of C-TiO₂ doped cellulose acetate nanocomposite film for removal of reactive Red-195. *Chem Eng Commun* 208:304–317. <https://doi.org/10.1080/00986445.2020.1712375>
- Poza-Nogueiras V, Rosales E, Pazos M, Sanromán MÁ (2018) Current advances and trends in electro-Fenton process using heterogeneous catalysts – A review. *Chemosphere* 201:399–416. <https://doi.org/10.1016/j.chemosphere.2018.03.002>
- Profeti LPR, Profeti D, Olivi P (2009) Pt–RuO₂ electrodes prepared by thermal decomposition of polymeric precursors as catalysts for direct methanol fuel cell applications. *Int J Hydrogen Energy* 34:2747–2757. <https://doi.org/10.1016/j.ijhydene.2009.01.011>
- Puvaneshwari N, Muthukrishnan J, Gunasekaran P (2006) Toxicity assessment and microbial degradation of azo dyes. *Ind J Exp Biol* 44(8):618–626
- Radjenovic J, Sedlak DL (2015) Challenges and opportunities for electrochemical processes as next-generation technologies for the treatment of contaminated water. *Environ Sci Technol* 49:11292–11302. <https://doi.org/10.1021/acs.est.5b02414>
- Rahmani AR, Godini K, Nematollahi D, Azarian G (2015) Electrochemical oxidation of activated sludge by using direct and indirect anodic oxidation. *Desalin Water Treat* 56:2234–2245. <https://doi.org/10.1080/19443994.2014.958761>
- Rahmani AR, Shabanloo A, Fazlzadeh M, Poureshgh Y (2020) Investigation of operational parameters influencing in treatment of dye from water by electro-Fenton process. *Desalin Water Treat* 57:24387–24394. <https://doi.org/10.1080/19443994.2016.1146918>
- Rajkumar D, Kim JG (2006) Oxidation of various reactive dyes with in situ electro-generated active chlorine for textile dyeing

- industry wastewater treatment. *J Hazard Mater* 136:203–212. <https://doi.org/10.1016/j.jhazmat.2005.11.096>
- Ramsay JA, Nguyen T (2002) Decoloration of textile dyes by *Trametes versicolor* and its effect on dye toxicity. *Biotechnol Lett* 24:1757–1761. <https://doi.org/10.1023/A:1020644817514>
- Ramya M, Karthika M, Selvakumar R et al (2017) A facile and efficient single step ball milling process for synthesis of partially amorphous Mg-Zn-Ca alloy powders for dye degradation. *J Alloys Compd* 696:185–192. <https://doi.org/10.1016/j.jallcom.2016.11.221>
- Ribeiro J, de Andrade AR (2006) Investigation of the electrical properties, charging process, and passivation of $\text{RuO}_2\text{-Ta}_2\text{O}_5$ oxide films. *J Electroanal Chem* 592:153–162. <https://doi.org/10.1016/j.jelechem.2006.05.004>
- Rosales E, Pazos M, Sanroman MA (2012) Advances in the electro-Fenton process for remediation of recalcitrant organic compounds. *Chem Eng Technol* 35:609–617. <https://doi.org/10.1002/ceat.201100321>
- Rosestolato D, Battaglin G, Ferro S (2014) Electrochemical properties of stoichiometric RuN film prepared by rf-magnetron sputtering: a preliminary study. *Electrochem Commun* 49:9–13. <https://doi.org/10.1016/j.elecom.2014.09.019>
- Roshini PS, Gandhimathi R, Ramesh ST, Nidheesh PV (2017) Combined electro-fenton and biological processes for the treatment of industrial textile effluent: mineralization and toxicity analysis. *J Hazardous Toxic Radioact Waste* 21:04017016. [https://doi.org/10.1061/\(ASCE\)HZ.2153-5515.0000370](https://doi.org/10.1061/(ASCE)HZ.2153-5515.0000370)
- Ruiz EJ, Arias C, Brillas E et al (2011) Mineralization of Acid Yellow 36azo dye by electro-Fenton and solar photoelectro-Fenton processes with a boron-doped diamond anode. *Chemosphere* 82:495–501. <https://doi.org/10.1016/j.chemosphere.2010.11.013>
- Sala M, Gutiérrez-Bouzán MC (2014) Electrochemical treatment of industrial wastewater and effluent reuse at laboratory and semi-industrial scale. *J Clean Prod* 65:458–464. <https://doi.org/10.1016/j.jclepro.2013.08.006>
- Salazar R, Gallardo-Arriaza J, Vidal J et al (2019) Treatment of industrial textile wastewater by the solar photoelectro-Fenton process: Influence of solar radiation and applied current. *Sol Energy* 190:82–91. <https://doi.org/10.1016/j.solener.2019.07.072>
- Salazar R, Campos S, Martínez J et al (2022) New development of a solar electrochemical raceway pond reactor for industrial wastewater treatment. *Environ Res* 212:113553. <https://doi.org/10.1016/j.envres.2022.113553>
- Salazar-Banda GR, de Santos G, OS, Duarte Gonzaga IM, et al (2021) Developments in electrode materials for wastewater treatment. *Curr Opin Electrochem* 26:100663. <https://doi.org/10.1016/j.coelec.2020.100663>
- Sandoval MA, Zúñiga-Mallea N, Espinoza LC et al (2019) Decolorization and degradation of a mixture of industrial Azo Dyes by anodic oxidation using a $\text{Ti/Ru}_0.3\text{Ti}_0.7\text{O}_2$ (DSA- Cl_2) electrode. *ChemistrySelect* 4:13856–13866. <https://doi.org/10.1002/slct.201903150>
- Santos DHS, Duarte JLS, Tavares MGR et al (2020) Electrochemical degradation and toxicity evaluation of reactive dyes mixture and real textile effluent over DSA® electrodes. *Chem Eng Proc Proc Intensif* 153:107940. <https://doi.org/10.1016/j.cep.2020.107940>
- Sathishkumar K, Sathiyaraj S, Parthipan P et al (2017) Electrochemical decolorization of methyl red by $\text{RuO}_2\text{-IrO}_2\text{-TiO}_2$ electrode and biodegradation with *Pseudomonas stutzeri* MN1 and *Acinetobacter baumannii* MN3: an integrated approach. *Chemosphere* 183:204–211. <https://doi.org/10.1016/j.chemosphere.2017.05.087>
- Saxena P, Ruparelia J (2019) Influence of supporting electrolytes on electrochemical treatability of reactive black 5 using dimensionally stable Anode. *J Inst Eng Ser A* 100:299–310. <https://doi.org/10.1007/s40030-019-00360-4>
- Scalbi S, Tarantini M, Mattioli D (2005) Efficient use of water in the textile finishing industry.
- Selvaraj V, Karthika TS, Mansiya C, Alagar M (2020) An over review on recently developed techniques, mechanisms and intermediate involved in the advanced azo dye degradation for industrial applications. *J Mol Struct* 1224:129195. <https://doi.org/10.1016/j.molstruc.2020.129195>
- Sennaoui A, Alahiane S, Sakr F et al (2018) Advanced oxidation of reactive yellow 17 Dye: a comparison between fenton, photo-fenton, electro-fenton, anodic oxidation and heterogeneous photocatalysis processes. *Port Electrochim Acta* 36:163–178. <https://doi.org/10.4152/pea.201803163>
- Setayesh SR, Nazari P, Maghbool R (2020) Engineered $\text{FeVO}_4/\text{CeO}_2$ nanocomposite as a two-way superior electro-Fenton catalyst for model and real wastewater treatment. *J Environ Sci* 97:110–119. <https://doi.org/10.1016/j.jes.2020.04.035>
- Siedlecka EM, Ofiarska A, Borzyszkowska AF et al (2018) Cytostatic drug removal using electrochemical oxidation with BDD electrode: Degradation pathway and toxicity. *Water Res* 144:235–245. <https://doi.org/10.1016/j.watres.2018.07.035>
- Singh RP, Singh PK, Gupta R, Singh RL (2019) Treatment and recycling of wastewater from textile industry. *Advances in biological treatment of industrial waste water and their recycling for a sustainable future*. Springer, Singapore, pp 225–266
- Sirés I, Brillas E (2021) Upgrading and expanding the electro-Fenton and related processes. *Curr Opin Electrochem* 27:100686. <https://doi.org/10.1016/j.coelec.2020.100686>
- Sirés I, Brillas E, Oturan MA et al (2014) Electrochemical advanced oxidation processes: today and tomorrow. *A Rev Environ Sci Pollut Res* 21:8336–8367. <https://doi.org/10.1007/s11356-014-2783-1>
- Solano AMS, Garcia-Segura S, Martínez-Huitile CA, Brillas E (2015) Degradation of acidic aqueous solutions of the diazo dye Congo Red by photo-assisted electrochemical processes based on Fenton's reaction chemistry. *Appl Catal B Environ* 168–169:559–571. <https://doi.org/10.1016/j.apcatb.2015.01.019>
- Soni BD, Ruparelia JP (2013) Decolourization and mineralization of Reactive black-5 with transition metal oxide coated electrodes by electrochemical oxidation. *Procedia Eng* 51:335–341. <https://doi.org/10.1016/j.proeng.2013.01.046>
- Soni BD, Patel UD, Agrawal A, Ruparelia JP (2020) Electrochemical destruction of RB5 on $\text{Ti/PtOx-RuO}_2\text{-SnO}_2\text{-Sb}_2\text{O}_5$ electrodes: a comparison of two methods for electrode preparation. *Int J Environ Sci Technol* 17:903–916. <https://doi.org/10.1007/s13762-019-02393-5>
- Steter JR, Brillas E, Sirés I (2016) On the selection of the anode material for the electrochemical removal of methylparaben from different aqueous media. *Electrochim Acta* 222:1464–1474. <https://doi.org/10.1016/j.electacta.2016.11.125>
- Subba Rao AN, Venkatarangaiah VT (2014) Metal oxide-coated anodes in wastewater treatment. *Environ Sci Pollut Res* 21:3197–3217. <https://doi.org/10.1007/s11356-013-2313-6>
- Sudha M, Saranya A, Selvakumar G, Sivakumar N (2014) Microbial degradation of azo dyes: a review. *Int J Curr Microbiol Appl Sci* 3:670–690. chrome-extension://efaidnbmnnnibpcajpcglclefindmkaj/<https://www.ijcmas.com/vol-3-2/M.Sudha,%20et%20al.pdf>
- Sun Y, Pignatello JJ (1993) Photochemical reactions involved in the total mineralization of 2,4-D by iron(3+)/hydrogen peroxide/UV. *Environ Sci Technol* 27:304–310. <https://doi.org/10.1021/es00039a010>
- Tang Y, He D, Guo Y et al (2020) Electrochemical oxidative degradation of X-6G dye by boron-doped diamond anodes: Effect of operating parameters. *Chemosphere* 258:127368. <https://doi.org/10.1016/j.chemosphere.2020.127368>

- Titchou FE, Zazou H, Afanga H et al (2021a) An overview on the elimination of organic contaminants from aqueous systems using electrochemical advanced oxidation processes. *J Water Process Eng* 41:102040. <https://doi.org/10.1016/j.jwpe.2021a.102040>
- Titchou FE, Zazou H, Afanga H et al (2021b) Electro-Fenton process for the removal of Direct Red 23 using BDD anode in chloride and sulfate media. *J Electroanal Chem* 897:115560. <https://doi.org/10.1016/j.jelechem.2021b.115560>
- Tomaz, A. T., Barthus, R. C., Costa, C. R., Ribeiro, J. (2022) Descontaminação de Águas Residuais Contendo Poluentes Orgânicos: Uma Revisão, *in press*. Doi: <https://doi.org/10.21577/1984-6835.20220076>.
- Tunç Ö, Tanacı H, Aksu Z (2009) Potential use of cotton plant wastes for the removal of Remazol Black B reactive dye. *J Hazard Mater* 163:187–198. <https://doi.org/10.1016/j.jhazmat.2008.06.078>
- Vaghela SS, Jethva AD, Mehta BB et al (2005) Laboratory Studies of Electrochemical Treatment of Industrial Azo Dye Effluent. *Environ Sci Technol* 39:2848–2855. <https://doi.org/10.1021/es035370c>
- Valero D, García-García V, Expósito E et al (2014) Electrochemical treatment of wastewater from almond industry using DSA-type anodes: Direct connection to a PV generator. *Sep Purif Technol* 123:15–22. <https://doi.org/10.1016/j.seppur.2013.12.023>
- Vasconcellos M, de Lourdes S, Luiz RG, Silva C-S, Fajardo AS, Garcia-Segura S, Ribeiro J (2021) Dimensionally stable anode based sensor for urea determination via linear sweep voltammetry. *Sensors* 21:3450–3460. <https://doi.org/10.3390/s21103450>
- Vasconcelos VM, Ponce-de-León C, Nava JL, Lanza MRV (2016) Electrochemical degradation of RB-5 dye by anodic oxidation, electro-Fenton and by combining anodic oxidation–electro-Fenton in a filter-press flow cell. *J Electroanal Chem* 765:179–187. <https://doi.org/10.1016/j.jelechem.2015.07.040>
- Vasconcelos VM, Ponce-de-León C, Rosiwal SM, Lanza MRV (2019) Electrochemical degradation of reactive blue 19 dye by combining boron-doped diamond and reticulated vitreous carbon electrodes. *ChemElectroChem* 6:3516–3524. <https://doi.org/10.1002/celec.201900563>
- Waghmode TR, Kurade MB, Govindwar SP (2011) Time dependent degradation of mixture of structurally different azo and non azo dyes by using *Galactomyces geotrichum* MTCC 1360. *Int Biodeterior Biodegradation* 65:479–486. <https://doi.org/10.1016/j.ibiod.2011.01.010>
- Wakrim A, Zaroual Z, El Ghachtouli S et al (2022) Treatment and degradation of Azo dye waste industry by electro-fenton process. *Phys Chem Res*. <https://doi.org/10.22036/PCR.2022.315931.1991>
- Wang R (2022) Application of boron doped diamond for electro-Fenton and photoelectro-Fenton decolorization of azo dye from dye-containing wastewater: Acid Red 1. *Int J Electrochem Sci*. <https://doi.org/10.20964/2022a.02.45>
- Xiao H, Wu M, Zhao G (2015) Electrocatalytic oxidation of cellulose to gluconate on carbon aerogel supported gold nanoparticles anode in alkaline medium. *Catalysts*. <https://doi.org/10.3390/catal6010005>
- Yang C, Wang D, Tang Q, Sun Y (2017) Decoloration of azo dye methyl orange by a novel electro-Fenton internal circulation batch reactor. *J Adv Oxid Technol*. <https://doi.org/10.1515/jaots-2016-0196>
- Zazou H, Oturan N, Sönmez Çelebi M et al (2019) Cold incineration of 1,2-dichlorobenzene in aqueous solution by electrochemical advanced oxidation using DSA/Carbon felt, Pt/Carbon felt and BDD/Carbon felt cells. *Sep Purif Technol* 208:184–193. <https://doi.org/10.1016/j.seppur.2018.03.030>
- Zhang J, Zhang Y, Quan X et al (2013) Enhanced anaerobic digestion of organic contaminants containing diverse microbial population by combined microbial electrolysis cell (MEC) and anaerobic reactor under Fe (III) reducing conditions. *Bioresour Technol* 136:273–280. <https://doi.org/10.1016/j.biortech.2013.02.103>
- Zhao H, Qian L, Guan X et al (2016) Continuous bulk FeCuC aerogel with ultradispersed metal nanoparticles: an efficient 3D heterogeneous electro-Fenton cathode over a wide range of pH 3–9. *Environ Sci Technol* 50:5225–5233. <https://doi.org/10.1021/acs.est.6b00265>
- Zhou M, Särkkä H, Sillanpää M (2011) A comparative experimental study on methyl orange degradation by electrochemical oxidation on BDD and MMO electrodes. *Sep Purif Technol* 78:290–297. <https://doi.org/10.1016/j.seppur.2011.02.013>
- Zou S, Yuan H, Childress A, He Z (2016) Energy consumption by recirculation: a missing parameter when evaluating forward osmosis. *Environ Sci Technol* 50:6827–6829. <https://doi.org/10.1021/acs.est.6b02849>

Publisher's Note Springer Nature remains neutral with regard to jurisdictional claims in published maps and institutional affiliations.

Springer Nature or its licensor (e.g. a society or other partner) holds exclusive rights to this article under a publishing agreement with the author(s) or other rightsholder(s); author self-archiving of the accepted manuscript version of this article is solely governed by the terms of such publishing agreement and applicable law.